

INVESTIGATION OF OLIGO(BENZOXAZABOROLE)S DERIVED FROM ALKYL-  
LINKED BIS(AMINOPHENOL)S

---

A Thesis

Presented to

The Faculty of the Department of Chemistry

Sam Houston State University

---

In Partial Fulfillment

of the Requirements for the Degree of

Master of Science

---

by

Ahangama Munasinghage Thusharika Muthumali

May, 2021

INVESTIGATION OF OLIGO(BENZOXAZABOROLE)S DERIVED FROM ALKYL-  
LINKED BIS(AMINOPHENOL)S

by

Ahangama Munasinghage Thusharika Muthumali

---

APPROVED:

Dustin E. Gross, PhD  
Thesis Director

Christopher E. Hobbs, PhD  
Committee Member

Tarek Trad, PhD  
Committee Member

John B. Pascarella, PhD  
Dean, College of Science and Engineering  
Technology

## **DEDICATION**

To my husband, daughter, parents, and brother.

## ABSTRACT

Muthumali, Ahangama Munasinghage Thusharika, *Investigation of oligo(benzoxazaborole)s derived from alkyl-linked bis(aminophenol)s*. Master of Science (Chemistry), May, 2021, Sam Houston State University, Huntsville, Texas.

Boronate ester-based materials have gained significant research interest and utility because of their ability to be formed through dynamic covalent bonds (DCBs). This reversible nature has been shown to organize molecular building blocks into the most thermodynamically stable structures such as linear polymers, nanotubes, macrocycles, and covalent organic frameworks (COFs).

Previously, we reported the synthesis of simple boronate ester derivatives, benzoxazaboroles, using 2-(alkylamino)phenols and diboronic acids. However, the synthesis of benzoxazaboroles derived from bis(aminophenol)s is less explored. There is a possibility to yield macrocycles along with the linear polymers due to the ditopic functionality of the starting materials and an equilibrium between ring and chain structures may exist.

In this research, we have synthesized investigated oligo(benzoxazaborole)s derived from alkyl-linked bis(aminophenol)s by both experimental and computational methods. Characterization of these materials was carried out using  $^1\text{H}$  NMR,  $^{13}\text{C}$  NMR, IR spectroscopy techniques.  $^1\text{H}$  NMR results indicate that the polymers exhibit dynamic covalent nature under mild conditions. Furthermore, IR spectroscopic analysis reveals that the degree of polymerization is quite high for the polymers due to the absence of signals related to the starting materials.

The thermodynamic calculations predicted that the formation of benzoxazaboroles depends on the difference in the connectivity of the benzoxazaborole rings within the

structure. Additionally, those calculations predicted that the linear benzoxazaboroles are more favorable than the ring structures. However, the energy difference is less than 53 kJ/mol.

**KEY WORDS:** Boronate ester, Bis(aminophenol), Bis(benzoxazaborole)s, Oligo(benzoxazaborole)s, Ring-chain equilibrium, Computational methods

## ACKNOWLEDGEMENTS

First and foremost, I offer my sincerest gratitude to my supervisor Dr. Dustin E. Gross for supporting me throughout this journey with patience and knowledge and for his enormous guidance.

In addition, I gratefully acknowledge my committee members, Dr. Christopher Hobbs and Dr. Tarek Trad for their valuable thoughts towards the successful completion of this thesis.

I would like to thank Chamari Weththasinghe and Morgan Johnson for their great deal of support on IR spectrometer.

I would also like to express my heartfelt gratitude to all my colleagues in the Gross research group for their laboratory assistance.

I would like to extend my gratitude to all the faculty members of the department of chemistry for helping me in various ways to complete my thesis successfully. I would also like to thank Mrs. Rachell Haines for her everyday support.

I deeply thank my husband Suranga Premachandre and my parents for their unconditional trust, timely encouragement, and endless patience.

Finally, I would like to thank my colleagues and all who have supported me throughout this work.

## TABLE OF CONTENTS

	<b>Page</b>
DEDICATION .....	iii
ABSTRACT .....	iv
ACKNOWLEDGEMENTS .....	vi
TABLE OF CONTENTS.....	vii
LIST OF TABLES .....	ix
LIST OF FIGURES .....	x
CHAPTER I: INTRODUCTION .....	1
Dynamic Covalent Chemistry (DCvC).....	1
Covalent Organic Frameworks (COFs).....	5
Boronic Acids .....	7
Benzoxazaboroles .....	9
Aims of this Work .....	11
CHAPTER II: RESULTS AND DISCUSSION .....	13
Synthesis of Alkyl-Linked bis(aminophenol)s (3a-c).....	13
Alkyl-Linked bis(benzoxazaborole) 6a .....	16
Alkyl-Linked bis(benzoxazaborole) 6c .....	19
Poly(benzoxazaborole) 8 .....	24
Poly(benzoxazaborole) 9 .....	28
Melting Point Analysis of Benzoxazaboroles.....	33
FTIR Analysis of Benzoxazaboroles .....	34

Computational Studies on the Synthesis and Ring–Chain Equilibrium of Poly(benzoxazaborole)s.....	38
CHAPTER III: CONCLUSIONS.....	45
CHAPTER IV: EXPERIMENTAL SECTION.....	47
REFERENCES .....	56
APPENDIX A.....	62
APPENDIX B.....	68
VITA.....	70

## LIST OF TABLES

Table		Page
1	Melting point data for <b>3a</b> , <b>7</b> , <b>3a+7</b> and polymer <b>8</b> .....	33
2	Melting point data for <b>3c</b> , <b>7</b> , <b>3c+7</b> and polymer <b>9</b> .....	34
3	Computational results for oligo(benzoxazaborole)s <b>8a-g</b> .....	39
4	Computational results for oligo(benzoxazaborole)s <b>9a-g</b> .....	40
5	$\Delta G$ calculations per benzoxazaborole ring for oligo(benzoxazaboroles)s.....	41
6	Predicted $\Delta G_{\text{formation}}$ of benzoxazaboroles for oligo(benzoxazaborole)s <b>8a-g</b> . ....	42
7	Predicted $\Delta G_{\text{formation}}$ of benzoxazaboroles for oligo(benzoxazaborole)s <b>9a-g</b> . ....	44

## LIST OF FIGURES

Figure	Page
1 Oligomer growth and ring-chain equilibria during dynamic covalent polymerization (DCvP).....	2
2 $\beta$ -hydroxyl ester-based transesterification. ....	2
3 Reversible metathesis reaction of aromatic disulfides.....	2
4 Reversible metathesis reaction of imines.....	3
5 Dynamic boronate ester bond formation through condensation. ....	3
6 Boronate ester based macrocycles obtained by the condensation reaction of bis-catechols with benzene diboronic acid. ....	3
7 Boronic ester based molecular cage in a [6+3+2] reaction of 4-formylphenylboronic acid, pentaerythritol, and tris(2-aminoethyl)amine.....	4
8 Boronate ester based vitrimers showing self-healing properties. ....	4
9 Dendritic nanostructures based on [4+4] type self-assembly of formylphenylboronic acids with 2,3-dihydroxypyridine .....	5
10 Formation of COF-1 via self-condensation of diboronic acids. ....	6
11 Formation of COF-5 via the co-condensation of diboronic acids with HHTP. ....	7
12 Formation of a dioxaborole from phenylboronic acid and catechol. ....	8
13 Formation of benzodiazaborole from phenylboronic acid and 1,2-phenylenediamine. ....	8
14 Synthesis of boronate ester-based poly(dioxaborole)s. ....	8
15 Synthesis of boronate ester-based poly(diazaborole)s.....	9
16 Formation of an oxazaborole from phenylboronic acid and 2-aminophenol.....	9

17	Synthesis of the bis(benzoxazaborole).....	10
18	Reported methods for the synthesis of the N-alkyl-linked bis(aminophenols).....	11
19	Synthesis of alkyl-linked bis(aminophenols) ( <b>3a-c</b> ).....	13
20	<sup>1</sup> H NMR spectrum of bis(aminophenol) <b>3a</b> .....	14
21	<sup>1</sup> H NMR spectrum of the product from the reaction between 2-aminophenol ( <b>1</b> ) and 1,4-dibromobutane ( <b>2b</b> ).....	15
22	<sup>1</sup> H NMR spectrum of the purified product from the reaction between 2- aminophenol ( <b>1</b> ) and 1,4-bis(bromomethyl)benzene ( <b>2c</b> ). ....	16
23	Synthesis of propane-1,3-bis(benzoxazaborole) ( <b>6a</b> ) from the reaction of propane-1,3-bis(aminophenol) ( <b>3a</b> ) and phenylboronic acid ( <b>5</b> ).....	16
24	Formation of boroxine <b>5a</b> . ....	17
25	The <sup>1</sup> H NMR spectrum of the condensation product from reaction between propane-1,3-bis(aminophenol) ( <b>3a</b> ) and phenylboronic acid ( <b>5</b> ).....	18
26	<sup>1</sup> H NMR spectrum of the reaction mixture of propane-1,3-bis(aminophenol) ( <b>3a</b> ) and phenylboronic acid ( <b>5</b> ).....	19
27	Synthesis of p-xylylene linked bis(benzoxazaborole) ( <b>6c</b> ) from the reaction between p-xylylene bis(aminophenol) ( <b>3c</b> ) and phenylboronic acid ( <b>5</b> ). ....	20
28	Stacked <sup>1</sup> H NMR spectra of the reaction mixture of p-xylylene bis(aminophenol) ( <b>3c</b> ) and phenylboronic acid ( <b>5</b> ).....	21
29	Stacked partial <sup>1</sup> H NMR spectra for the synthesis of p-xylylene bis(benzoxazaborole) ( <b>6c</b> ).....	22
30	Percent formation of bis(benzoxazaborole) <b>6c</b> over time. ....	23

31	Partial <sup>1</sup> H NMR spectrum of the product from the reaction between p-xylylene bis(aminophenol) ( <b>3c</b> ) and phenylboronic acid ( <b>5</b> ) from the solvent removal method. ....	24
32	Attempted synthesis of poly(benzoxazaborole) <b>8</b> from the reaction between bis(aminophenol) <b>3a</b> and diboronic acid <b>7</b> .....	25
33	NMR tube containing 1:1 ratio of propane-1,3-bis(aminophenol) ( <b>3a</b> ) and benzene diboronic acid ( <b>7</b> ).....	26
34	Stacked <sup>1</sup> H NMR spectra for the synthesis of poly(benzoxazaborole).....	27
35	The crystalline solid obtained from the reaction of propane-1,3-bis(aminophenol) ( <b>3a</b> ) and benzene diboronic acid ( <b>7</b> ).....	28
36	Synthesis of p-xylylene based poly(benzoxazaborole) ( <b>9</b> ) from the reaction between p-xylylene bis(aminophenol) ( <b>3c</b> ) and benzene diboronic acid ( <b>7</b> ).....	28
37	Stacked <sup>1</sup> H NMR spectra for the synthesis of poly(benzoxazaborole) <b>9</b> .....	29
38	Partial <sup>1</sup> H NMR spectrum for the synthesis of poly(benzoxazaborole) <b>9</b> .....	30
39	Partial <sup>1</sup> H NMR spectrum for the synthesis of poly(benzoxazaborole) <b>9</b> .....	31
40	White crystals from the reaction of p-xylylene bis(aminophenol) ( <b>3c</b> ) and benzene diboronic acid ( <b>7</b> ).....	31
41	Partial stacked <sup>1</sup> H NMR spectra for the hydrolysis of poly(benzoxazaborole) <b>9</b> with the addition of H <sub>2</sub> O .....	32
42	FTIR data for aminophenols <b>3a</b> , <b>3c</b> , phenylboronic acid ( <b>5</b> ), benzene diboronic acid ( <b>7</b> ).....	35
43	FTIR spectra of propane-1,3-bis(aminophenol) ( <b>3a</b> ), phenylboronic acid ( <b>5</b> ), and propane-1,3-bis(benzoxazaborole) ( <b>6a</b> ). ....	36

44	FTIR spectra of p-xylylene bis(aminophenol) ( <b>3c</b> ), phenylboronic acid ( <b>5</b> ), and p-xylylene bis(benzoxazaborole) ( <b>6b</b> ). .....	36
45	FTIR spectra of propane-1,3-bis(aminophenol) ( <b>3a</b> ), benzene diboronic acid ( <b>7</b> ), and propane-1,3-poly(benzoxazaborole) ( <b>8</b> ). .....	37
46	FTIR spectra of p-xylylene bis(aminophenol) ( <b>3c</b> ), benzene diboronic acid ( <b>7</b> ), and p-xylylene poly(benzoxazaborole) ( <b>9</b> ). .....	37
47	The optimized structures of linear and cyclic oligo(benzoxazaborole)s <b>8</b> . .....	39
48	The optimized structures of linear and cyclic oligo(benzoxazaborole)s <b>9</b> . .....	40

## CHAPTER I

### Introduction

#### Dynamic Covalent Chemistry (DCvC)

Dynamic covalent chemistry (DCvC) is an important aspect of supramolecular chemistry and has been shown to facilitate the dynamic formation of thermodynamically stable structures. It involves reversible covalent bond breaking and forming under suitable reaction conditions. Therefore, DCvC allows for error-checking and proofreading during synthesis, which enables the organization or reorganization of less thermodynamically stable products into more stable structures.<sup>1</sup> DCvC has been used extensively in material science, surface chemistry, catalysis, chemical biology, nanochemistry, and analytical sensing.<sup>2-6</sup>

To be a dynamic system, the lifetime of these covalent reversible bonds should be in the range of 1 ms to 1 min.<sup>7</sup> In most cases, the time required for DCvC reactions can be shortened by the addition of a catalyst or changing experimental conditions such as pH, solvent, temperature, etc.

During a dynamic covalent polymerization (DCvP), there is a possibility to yield stable cyclic structures in addition to typical acyclic oligomers, and under certain conditions, ring-chain equilibrium can exist between these structures (Figure 1).<sup>8</sup>

This ring-chain equilibrium is expected to depend on the geometry (directionality) and concentration of the monomers. It has been shown in other DCvP systems that high monomer concentration favors linear chain growth due to intermolecular processes and low monomer concentration favors the cyclic structures due to the more favorable intramolecular reactions.<sup>9</sup>

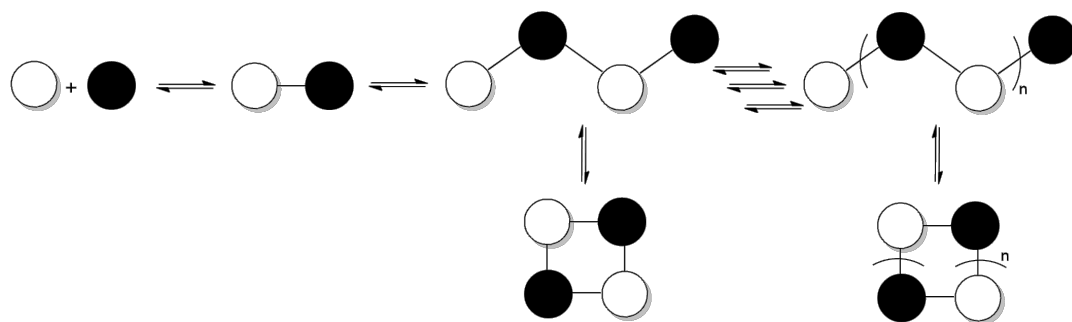


**Figure 1.** Oligomer growth and ring-chain equilibria during dynamic covalent polymerization (DCvP).

There are two main types of DCvC reactions: (1) exchange reactions and (2) formation of new functional groups such as condensation reactions. Symmetrical bonds such as carbon-carbon double bonds undergo self-exchange in olefin metathesis whereas some directional unsymmetrical bonds such as carbon-nitrogen or boron-oxygen need the combination of two different functional groups.<sup>10</sup> Various functional groups such as carboxylate esters (Figure 2), disulfides (Figure 3), imines (Figure 4), and boronate esters (Figure 5),<sup>10,11</sup> to name a few, have been investigated in the field of DCvC.<sup>1</sup>

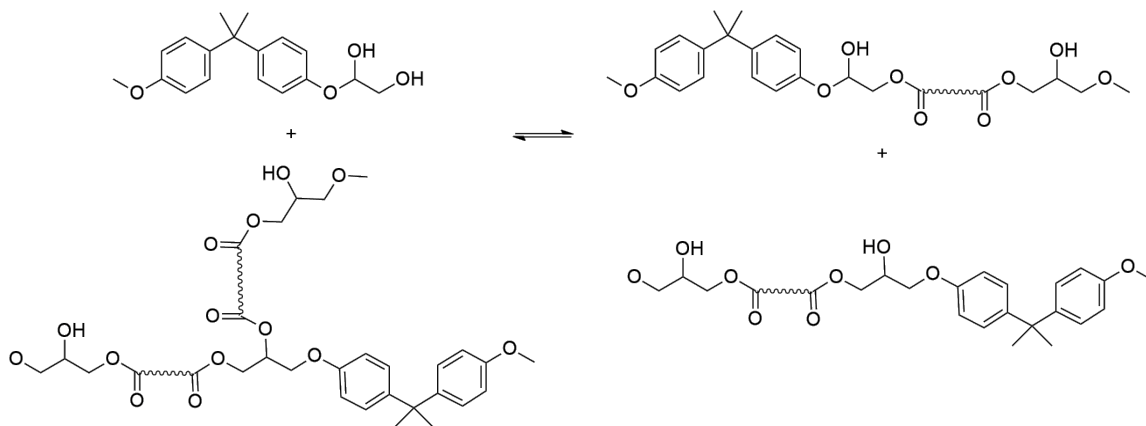


**Figure 2.**  $\beta$ -hydroxyl ester-based transesterification.<sup>12</sup>

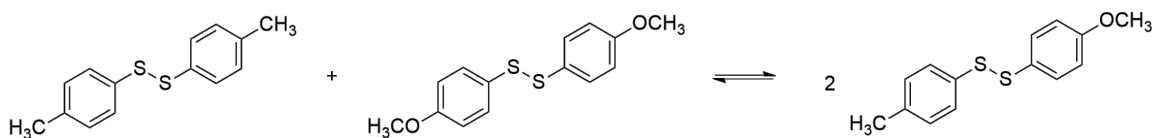


**Figure 3.** Reversible metathesis reaction of aromatic disulfides.<sup>13</sup>

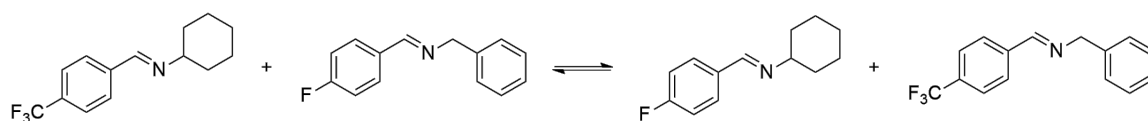


**Figure 4.** Reversible metathesis reaction of imines.<sup>14</sup>

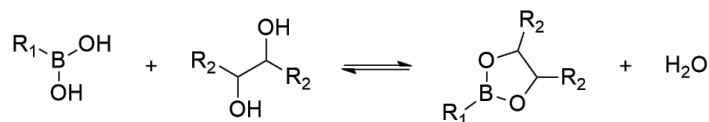


**Figure 5.** Dynamic boronate ester bond formation through condensation.

Dynamic covalent reactions involving boronic acids have long been utilized in the design of receptors<sup>15</sup> and sensors<sup>16</sup> and more recently this chemistry has been used for the construction of macrocycles (Figure 6),<sup>17</sup> 3D cages (Figure 7),<sup>18</sup> self-healing polymers (Figure 8),<sup>19</sup> dendrimers (Figure 9),<sup>20</sup> as well as covalent organic frameworks (COFs).<sup>21,22</sup>

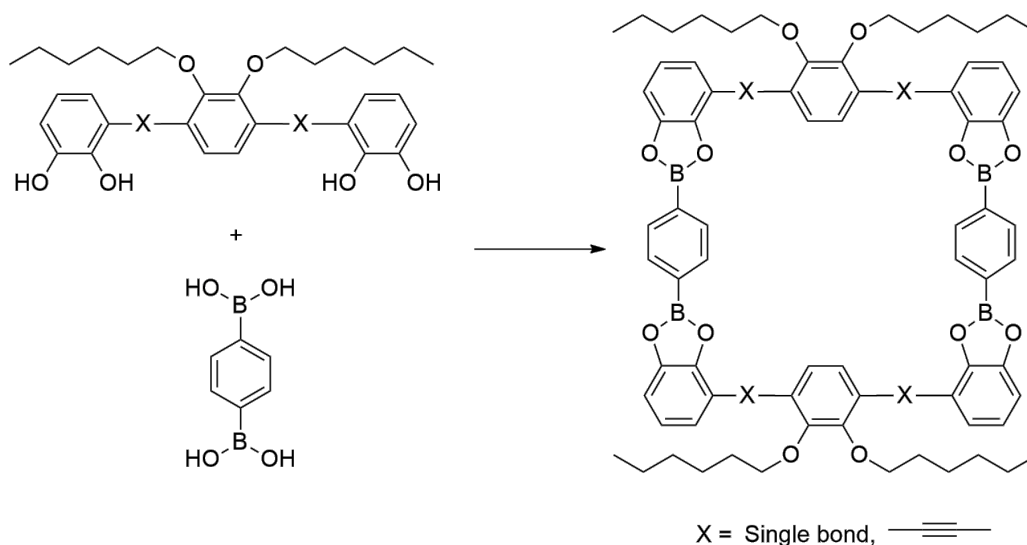


**Figure 6.** Boronate ester based macrocycles obtained by the condensation reaction of bis-catechols with benzene diboronic acid.<sup>23</sup>

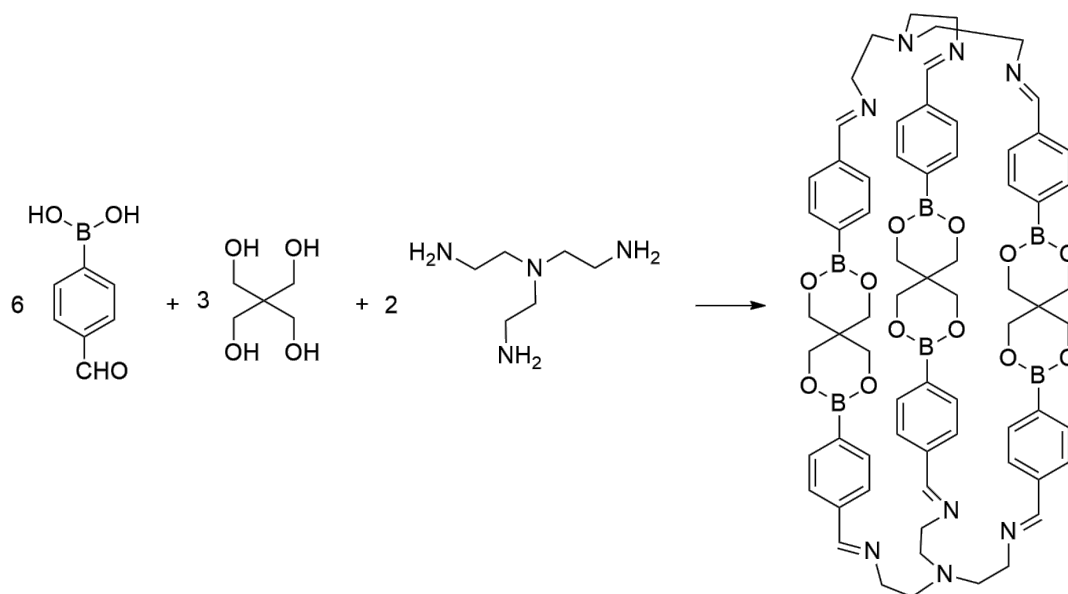


**Figure 7.** Boronic ester based molecular cage in a [6+3+2] reaction of 4-formylphenylboronic acid, pentaerythritol, and tris(2-aminoethyl)amine.<sup>18</sup>

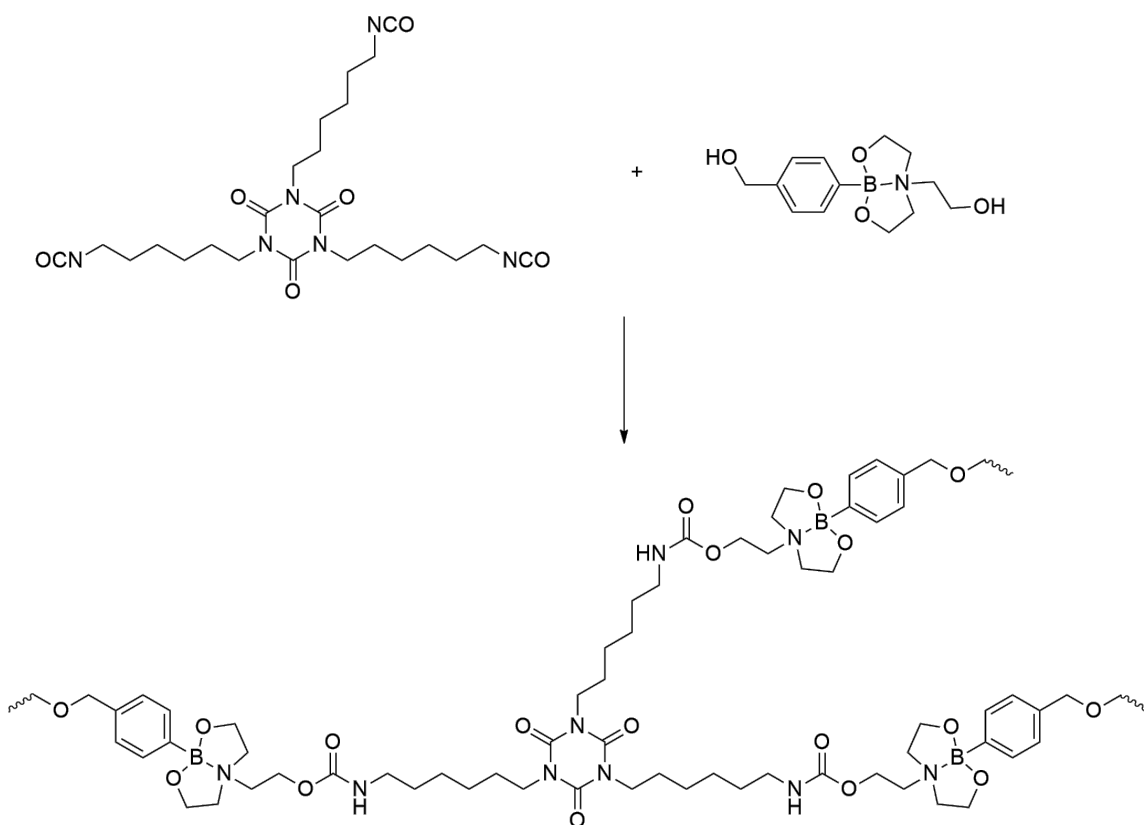


**Figure 8.** Boronate ester based vitrimers showing self-healing properties.<sup>24</sup>

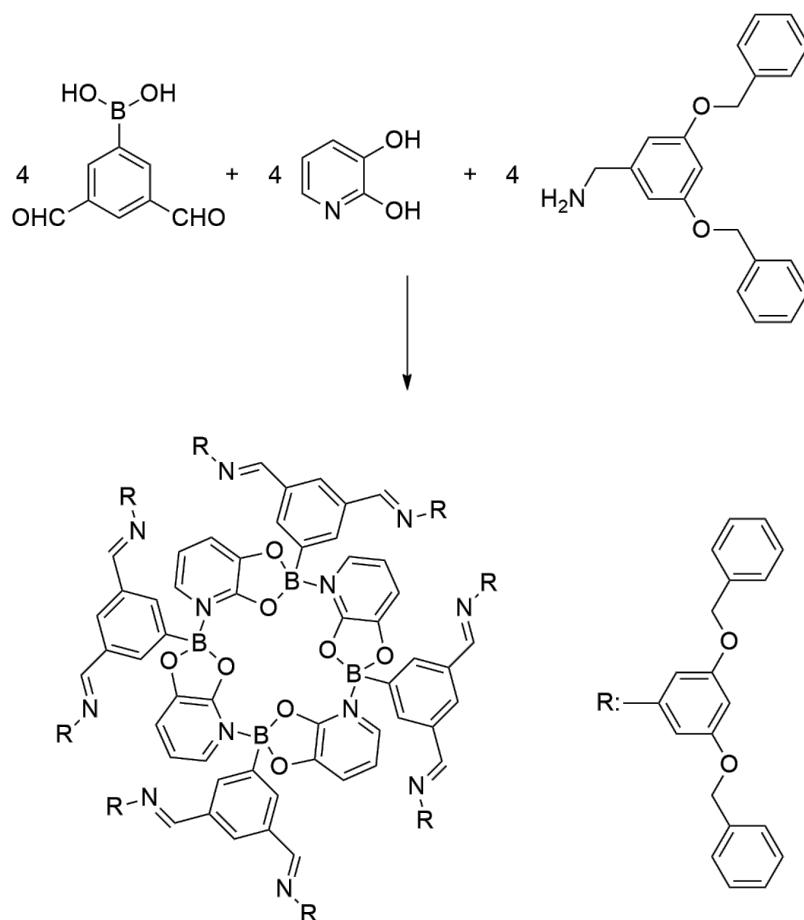


**Figure 9.** Dendritic nanostructures based on [4+4] type self-assembly of formylphenylboronic acids with 2,3-dihydroxypyridine.<sup>25</sup>

### Covalent Organic Frameworks (COFs)

Covalent organic frameworks (COFs) are an emerging class of crystalline, highly porous materials and have attracted attention for potential applications in gas storage and separation,<sup>21,26</sup> optoelectronics,<sup>27–29</sup> heterogeneous catalysis,<sup>30</sup> sensing,<sup>31</sup> and as charge carrier materials.<sup>32,33</sup> Unlike metal organic frameworks (MOFs), COFs are entirely constructed from light elements such as hydrogen, boron, nitrogen, carbon, and oxygen.<sup>22</sup> They are highly ordered extended organic architectures held together by strong covalent bonds. Depending on the connectivity and the geometry of the organic subunits, there are two main types of COFs, three-dimensional (3D) and two-dimensional (2D). In 2D COFs,

the organic units are linked into 2D layers that are stacked together via weak interactions such as  $\pi$ - $\pi$  interactions, hydrogen bonds, or van der Waals forces. In contrast, the building blocks in 3D COFs are all connected by covalent bonds.

The first synthesized 2D COF is COF-1, which was reported by Yaghi and co-workers in 2005.<sup>22</sup> It is based on the self-condensation of 1,4-benzenediboronic acid (BDDBA), which leads to the formation of the six-membered boroxine ( $B_3O_3$ ) ring by the removal of water (Figure 10). In the same report, they disclosed the synthesis of COF-5, via co-condensation of BDDBA with a trigonal building block hexahydroxytriphenylene (HHTP) (Figure 11).

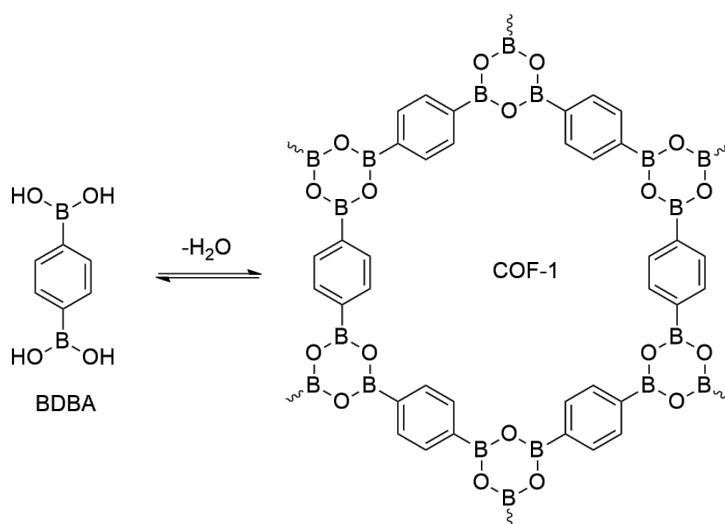


**Figure 10.** Formation of COF-1 via self-condensation of diboronic acids.

The first 3D COFs (termed COF-102, COF-103, COF-105, and COF-108) were reported by Yaghi and coworkers in 2007.<sup>34</sup> These were created by linking tetrahedral and trigonal planar building blocks together. To date, COF research is mainly focused on 2D systems due to problems with the synthesis and stability of 3D COFs.<sup>35</sup> Despite these problems, 3D COFs may be better suited for applications such as separation, storage, catalysis, guest incorporation, etc.

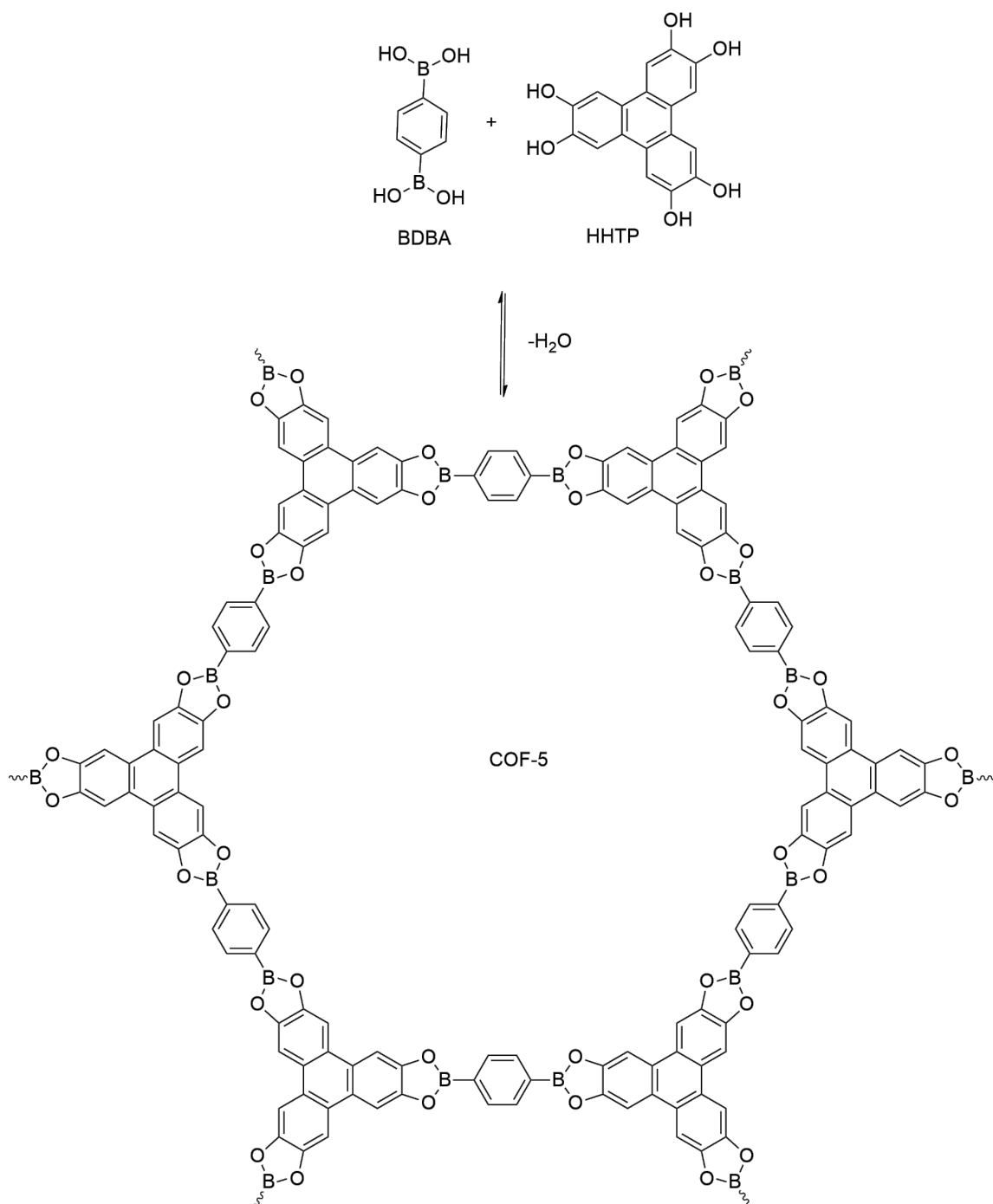


**Figure 11.** Formation of COF-5 via the co-condensation of diboronic acids with HHTP.

### Boronic Acids

Much of the unique properties of boronic acids arise from the low valence and empty p orbital of the boron atom, which enables them to accept electron density. This

allows for Lewis acid/base interactions, boroxine formation, boronate esterification, and hydrogen bonding.<sup>36</sup> The condensation of boronic acids with unsaturated 1,2-diols leads to the formation of cyclic boronate esters, which are also recognized as dioxaboroles (Figure 12).

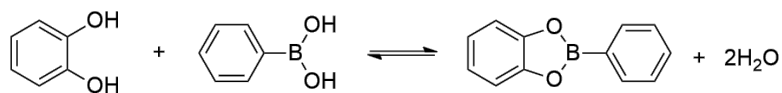


**Figure 12.** Formation of a dioxaborole from phenylboronic acid and catechol.

Similarly, the condensation of boronic acids with unsaturated 1,2-diamines leads to the formation of diazaboroles (Figure 13), which are structurally analogous to dioxaboroles. These compounds are strongly luminescent and have potential applications as electron conducting materials in electro-optical devices.<sup>37</sup>

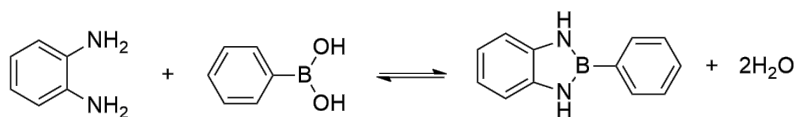


**Figure 13.** Formation of benzodiazaborole from phenylboronic acid and 1,2-phenylenediamine.

The synthesis of poly(dioxaborole)s using 9,9-dihexylfluorene-2,7-diboronic acid and pentaerythritol (Figure 14) by azeotropic removal of water was reported by Lavigne and coworkers.<sup>38</sup> To demonstrate the self-repairing property due to hydrolytic damage of these materials, the polymer was degraded by exposing it to water and then repaired by removing water under reduced pressure.

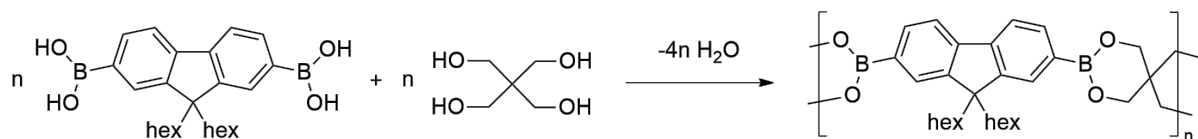


**Figure 14.** Synthesis of boronate ester-based poly(dioxaborole)s.

Marvel and coworkers reported the synthesis of several poly(benzodiazaborole)s using 3,3'-diaminobenzidine and diboronic esters (Figure 15). The diazaborole-based polymers synthesized from benzene diboronic esters showed good thermal stability.<sup>39</sup> The dynamic nature of these polymers was not reported.

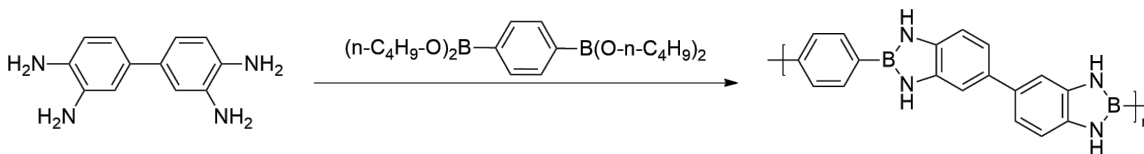


**Figure 15.** Synthesis of boronate ester-based poly(diazaborole)s.

### Benzoxazaboroles

Related to dioxaboroles and diazaboroles are oxazaboroles, which may possess overlapping properties and serve as molecular architecture building blocks similar to both the dioxo and diaza derivatives. The formation of oxazaboroles is possible through the condensation between boronic acids and unsaturated 2-aminoalcohols (Figure 16).<sup>40</sup>

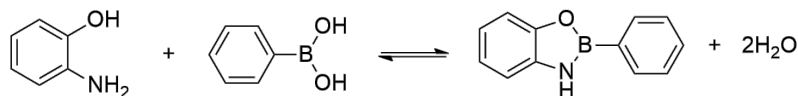


**Figure 16.** Formation of an oxazaborole from phenylboronic acid and 2-aminophenol.

In previous work, members of our research group have synthesized benzoxazaboroles, such as *N*-alkyl benzoxazaboroles and bis(benzoxazaborole)s and studied their dynamic covalent exchange properties (Figure 17).<sup>41,42</sup> However, it was found that bis(benzoxazaborole)s exhibited poor solubility in CDCl<sub>3</sub>. This issue was circumvented by preparing *N*-alkyl derivatives. In direct exchange reaction studies, it was found that benzoxazaboroles display similar stabilities to benzodioxaboroles. Furthermore, the stability of the *N*-alkyl benzoxazaboroles does not depend on the length of the alkyl chain.<sup>41,42</sup>

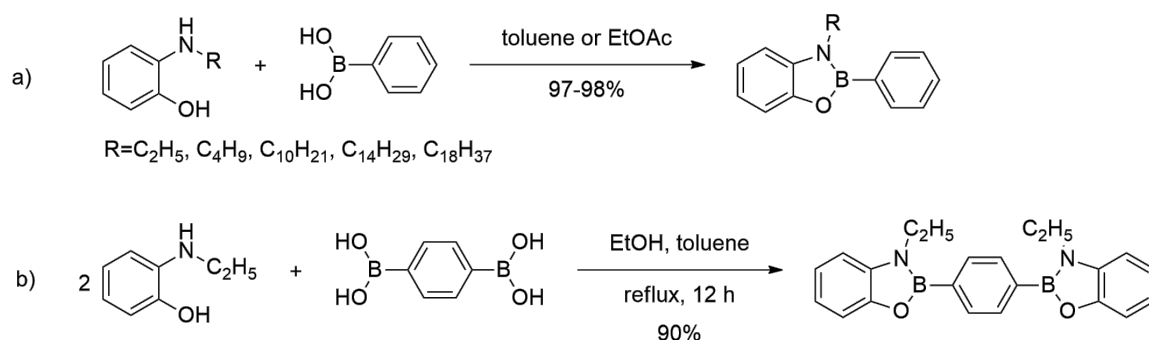


**Figure 17.** Synthesis of the benzoxazaboroles: (a) *N*-alkyl benzoxazaboroles and (b) bis(benzoxazaborole)s. The synthesis of an alkyl-linked bis(benzoxazaborole)s was reported by Barba and coworkers.<sup>43</sup>

The formation of this bis(benzoxazaborole) was possible by refluxing a bis(aminophenol) derivative and phenylboronic acid in xylenes (Figure 18).

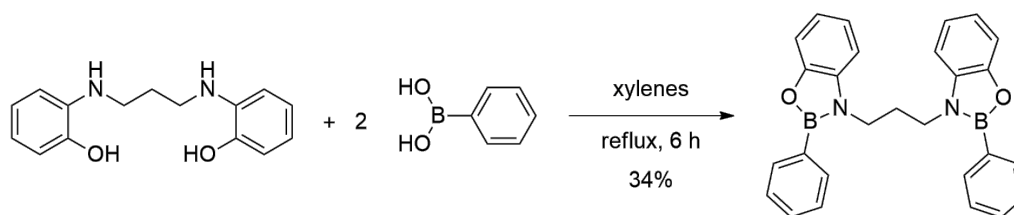


**Figure 18.** Synthesis of the bis(benzoxazaborole).

We envision that the condensation of bis(aminophenol)s with diboronic acids may result in oligo(benzoxazaborole)s, poly(benzoxazaborole)s, or potentially macrocycles due to the ditopic functionality of the starting materials. The properties of these materials can be modified by further functionalization of the linker on the bis(aminophenol).

Few approaches have been reported for the preparation of bis(aminophenol)s. The synthesis of bis(aminophenol) derivatives was first reported by Santillan and coworkers in 2000 by the reduction of the product resulting from the reaction between 2-aminophenol and glyoxal, using BH<sub>3</sub>-THF (Figure 19a).<sup>44</sup> A few years later, Barba and coworkers reported a different method of synthesis, in which the compound was synthesized by using 2-aminophenol and 1,3-dibromopropane in melt phase in a sealed tube (Figure 19b).<sup>43</sup> In

the same year, Gilbert and coworkers reported the synthesis of bis(aminophenol) with the phenyl group on the linker by reductive amination method, specifically the reaction between terephthalaldehyde and 2-aminophenol using sodium borohydride (Figure 19c).<sup>45</sup>

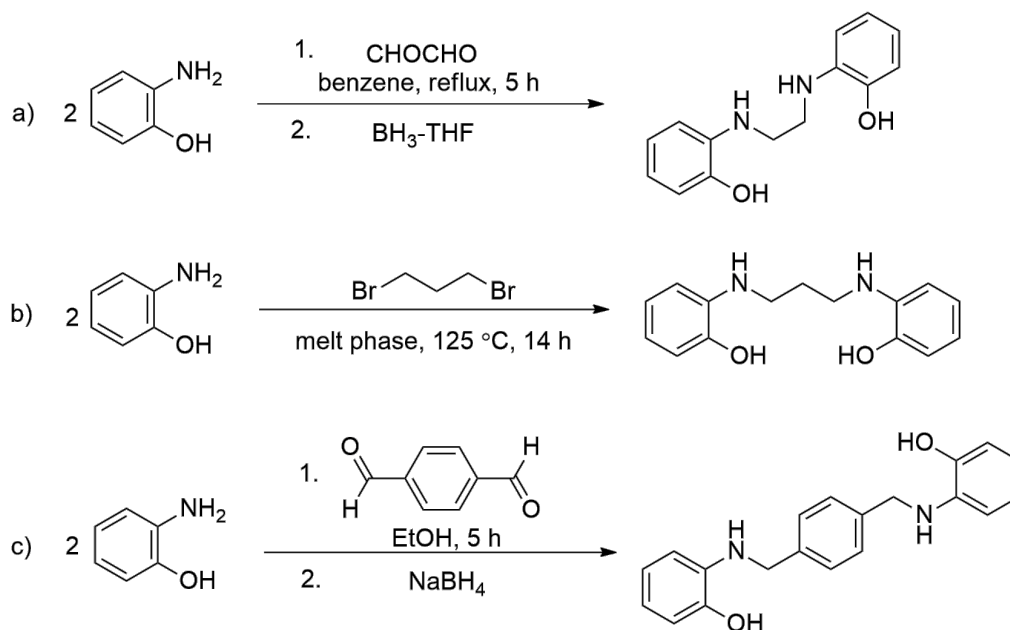


**Figure 19.** Reported methods for the synthesis of the *N*-alkyl-linked bis(aminophenols).

As described above, there are few bis(aminophenol) and one alkyl-linked benzoxazaborole system that have been reported so far. There has been no report of poly(benzoxazaborole)s.

### Aims of this Work

The main goal of this work is to synthesize poly(benzoxazaborole)s using alkyl-linked bis(aminophenols) and study the ring chain equilibrium of the products. To accomplish this, the synthesis of bis(aminophenols) is required by *N*-alkylation of *o*-aminophenol with alkyl dibromides or by reductive amination using dialdehydes and *o*-aminophenol. The synthesis of bis(benzoxazaborole)s and poly(benzoxazaborole)s was carried out either by mixing bis(aminophenols) and benzene boronic acid or benzene diboronic acid in common organic solvents. Computational studies of the products were

performed to obtain optimum geometries and thermodynamics of the formation of bis(benzoxazaborole)s and poly(benzoxazaborole)s. Finally, the polymerization/depolymerization and ring-chain equilibrium keep studied by NMR spectroscopy and computationally.

## CHAPTER II

## Results and Discussion

**Synthesis of Alkyl-Linked bis(aminophenols) (3a-c).** Using a similar method to that in the literature,<sup>43</sup> the synthesis of alkyl-linked bis(aminophenols) (**3a-c**) was attempted using 2-aminophenol (**1**) and alkyl dibromides (**2a-c**) in the melt phase. Three bis(aminophenol) derivatives were targeted using 1,3-dibromopropane (**2a**), 1,4-dibromobutane (**2b**), and 1,4-bis(bromomethyl)benzene (**2c**) as the dibromides (Figure 20).

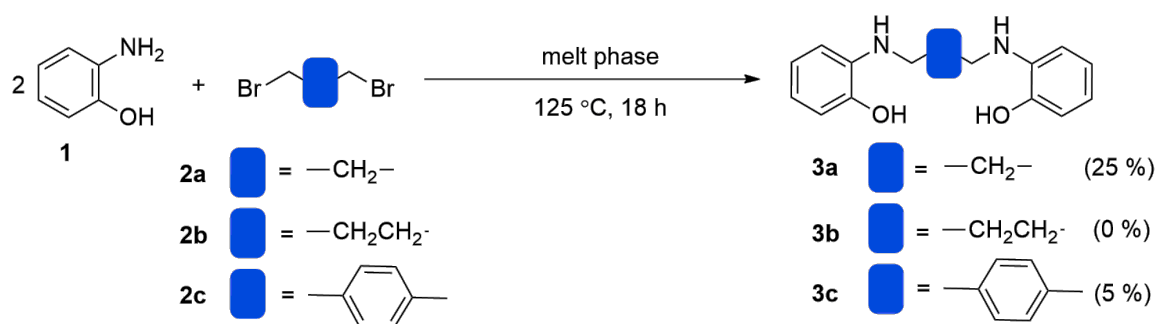


**Figure 20.** Synthesis of alkyl-linked bis(aminophenols) (**3a-c**).

The previously known<sup>43</sup> alkyl-linked bis(aminophenol) **3a** was purified and isolated (25% yield) using silica gel column chromatography. The propane-1,3-bis(aminophenol) (**3a**) was sparingly soluble in  $\text{CDCl}_3$ . However,  $\text{DMSO-}d_6$  was used to confirm the identity and purity of the isolated product by  $^1\text{H NMR}$  (Figure 21).

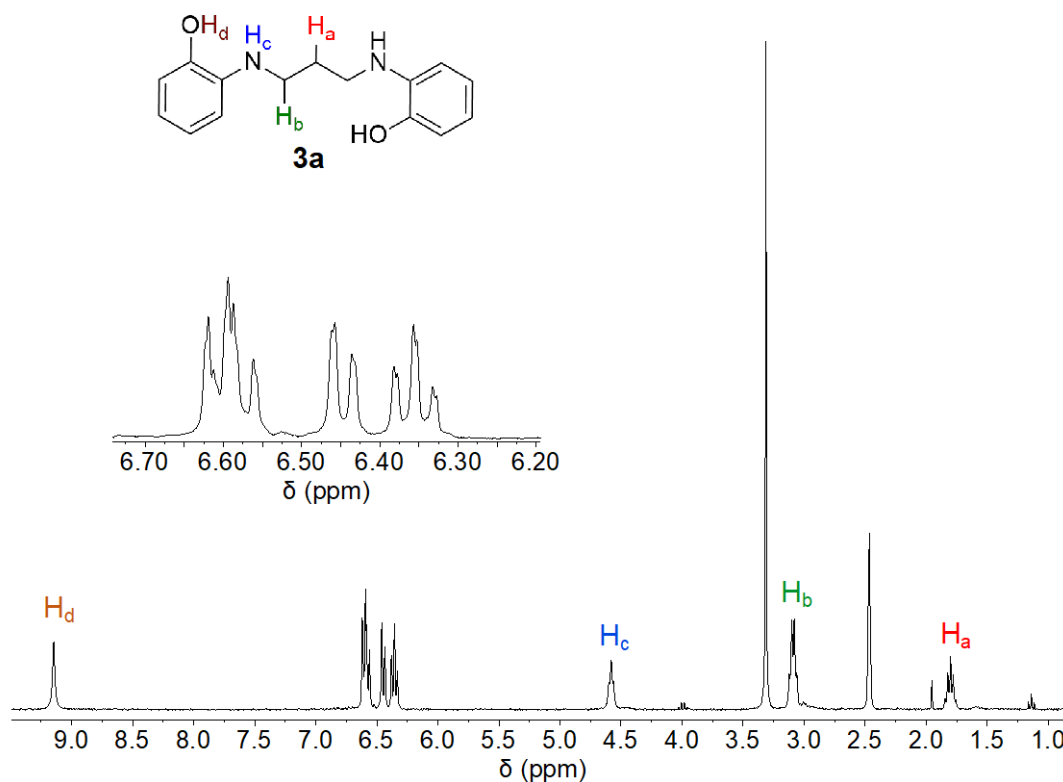


**Figure 21.**  $^1\text{H}$  NMR spectrum of bis(aminophenol) **3a** in  $\text{DMSO-}d_6$ .

Next, the synthesis of bis(aminophenol) **3b** was attempted and the product was purified using the same method that was used for bis(aminophenol) **3a**.  $^1\text{H}$  NMR spectroscopy was used to analyze the identity and purity of the isolated product (Figure 22). The obtained white solid was readily soluble in  $\text{CDCl}_3$ ; however, according to the  $^1\text{H}$  NMR data, the isolated product was determined to be a pyrrolidine product instead of the expected bis(aminophenol) **3b**. The presence of unreacted 2-aminophenol (**1**) in the crude reaction mixture also supported the formation of the pyrrolidine **4**. There was not an attempt to isolate the product or determine the percent yield due to the absence of the expected bis(aminophenol) product.

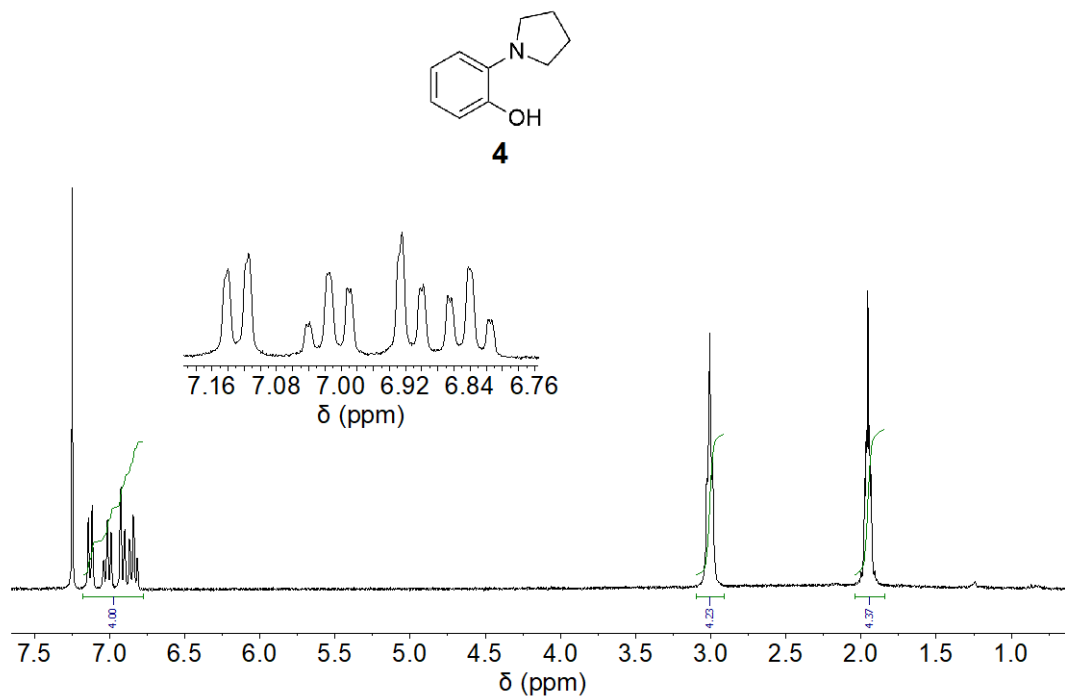


**Figure 22.**  $^1\text{H}$  NMR spectrum of the product from the reaction between 2-aminophenol (**1**) and 1,4-dibromobutane (**2b**) in  $\text{CDCl}_3$ .

The p-xylylene bis(aminophenol) (**3c**) was synthesized using a similar method to that of the bis(aminophenol) **3a** and was purified and isolated (5% unoptimized yield) using silica gel column chromatography. The bis(aminophenol) **3c**, was sparingly soluble in  $\text{CDCl}_3$  relative to the propane-1,3-bis(aminophenol) (**3a**). Therefore, to check the  $^1\text{H}$  NMR,  $\text{THF-}d_8$  was used to confirm the identity and purity of the isolated colorless solid (Figure 23).

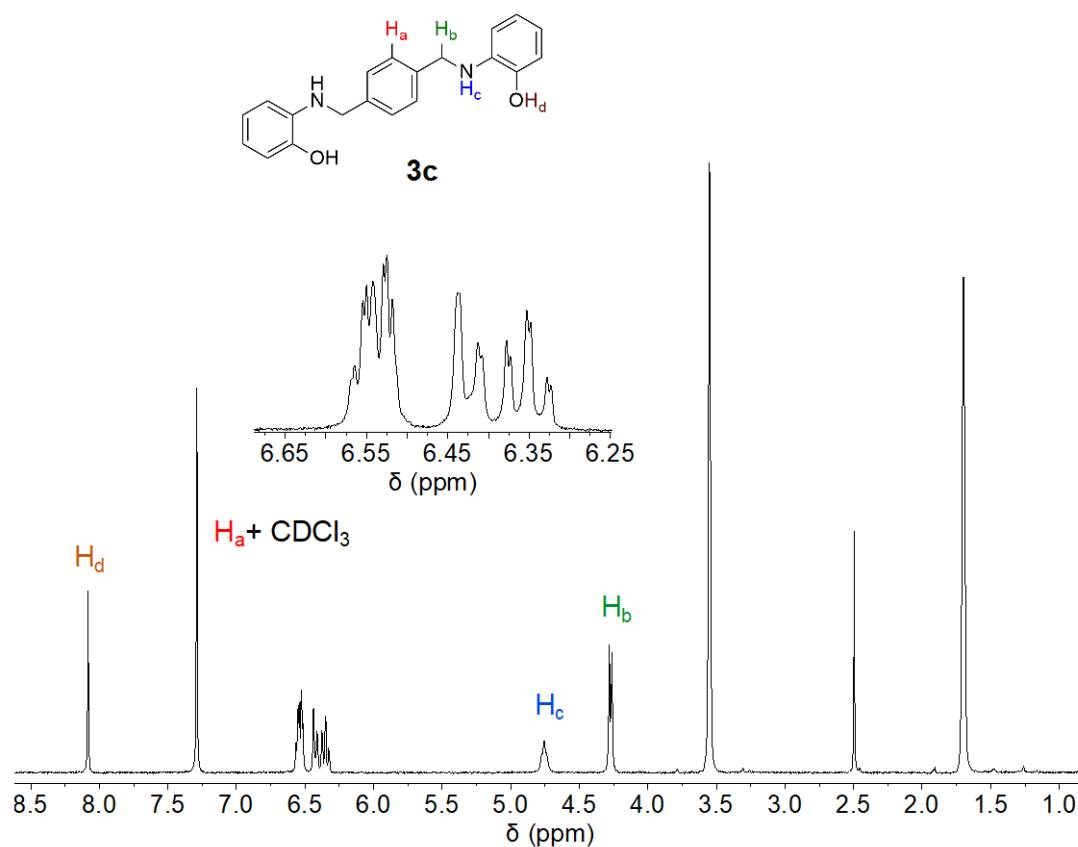


**Figure 23.**  $^1\text{H}$  NMR spectrum of the purified product from the reaction between 2-aminophenol (**1**) and 1,4-bis(bromomethyl)benzene (**2c**), in  $\text{THF-d}_8$ .

### Alkyl-Linked bis(benzoxazaborole) **6a**

The synthesis of alkyl-linked bis(benzoxazaborole)s has been reported by Barba and coworkers by refluxing a propane-1,3-bis(aminophenol) derivative (**3a**) and phenylboronic acid (**5**) in xylenes at 140 °C (Figure 24a).<sup>43</sup>

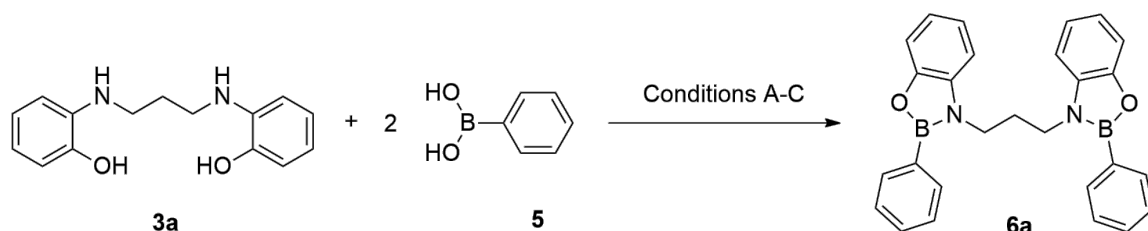


**Figure 24.** Synthesis of propane-1,3-bis(benzoxazaborole) (**6a**) from the reaction of propane-1,3-bis(aminophenol) (**3a**) and phenylboronic acid (**5**).; (a) reflux in xylylene, 140 °C (34%) (b) reflux in toluene, 110 °C (62%) (c)  $\text{CDCl}_3$ , 25 °C.

Similar to our previous work,<sup>41,42</sup> for the synthesis of bis(benzoxazaborole) **6a** we followed milder conditions than described in the literature.<sup>43</sup> Propane-1,3-bis(aminophenol) **3a** and phenylboronic acid (**5**) were refluxed for 9 h in toluene at 110 °C using a Dean-Stark trap (Figure 24b). The purpose of using a Dean-Stark trap is to remove water formed during the condensation reaction, thereby shifting the equilibrium towards the formation of **6a**. Additionally, the direct synthesis of bis(benzoxazaborole) **6a** was attempted by mixing the starting materials in CDCl<sub>3</sub> at room temperature (Figure 24c).<sup>46</sup>

The bis(benzoxazaborole) product **6a** from refluxing 1:2 ratio of bis(aminophenol) **3a** and phenylboronic acid (**5**) was analyzed using <sup>1</sup>H NMR. The spectrum (Figure 26) showed product **6a** along with the excess phenylboronic acid (**5**) and boroxine **5a**, the self-condensation product of phenylboronic acid (**5**) (Figure 25).

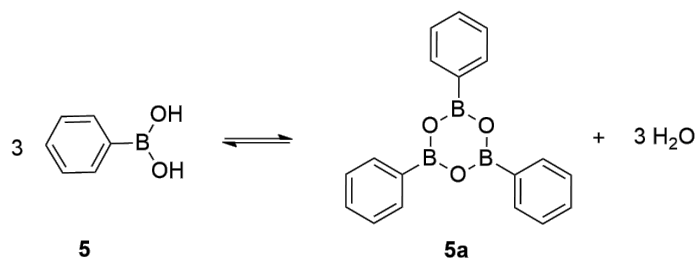


**Figure 25.** Formation of boroxine **5a**.

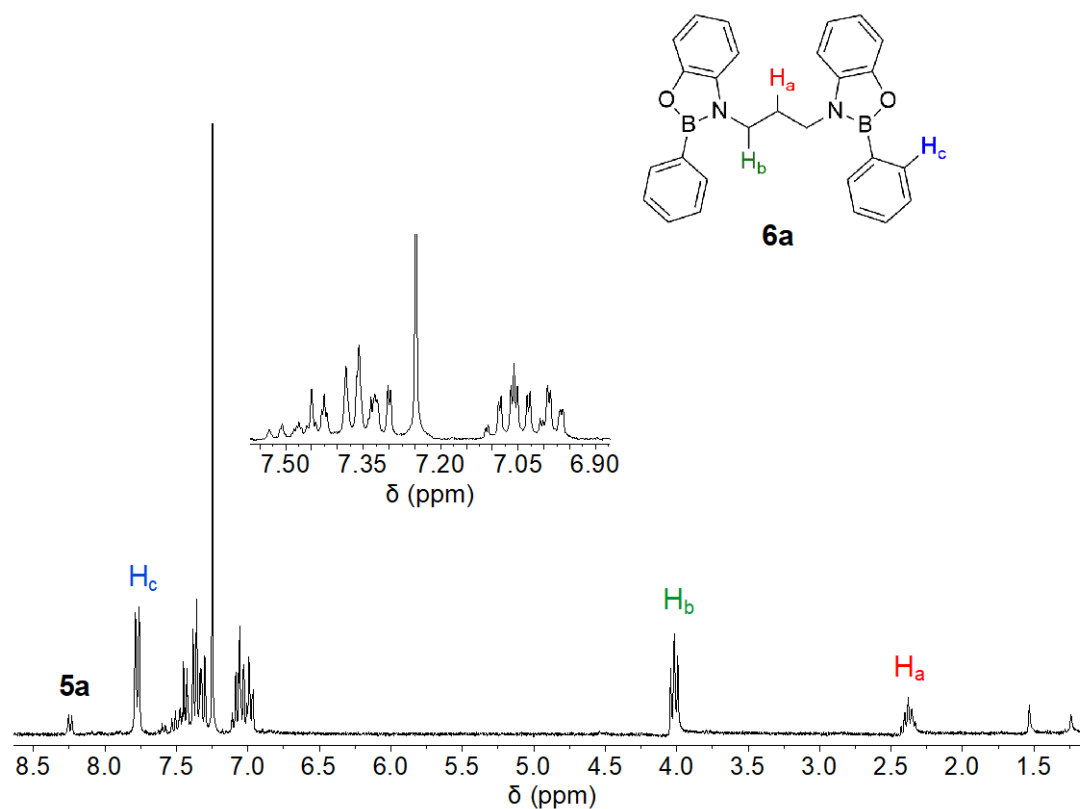


**Figure 26.** The  $^1\text{H}$  NMR spectrum of the condensation product from reaction between propane-1,3-bis(aminophenol) (**3a**) and phenylboronic acid (**5**), in refluxing toluene.

For the direct synthesis of propane-1,3-bis(benzoxazaborole) **6a**, a 1:2 ratio of propane-1,3-bis(aminophenol) (**3a**) and phenylboronic acid (**5**) were mixed in  $\text{CDCl}_3$  at room temperature. The formation of the product was supported by the presence of the corresponding  $^1\text{H}$  NMR signals (Figure 27). As in the previous method, the spectrum showed bis(benzoxazaborole) (**6a**), excess phenylboronic acid (**5**), and boroxine (**5a**). This result indicates that, even though the starting material **3a** is sparingly soluble in chloroform, the solubility of product **6a** may help to facilitate the forward reaction.

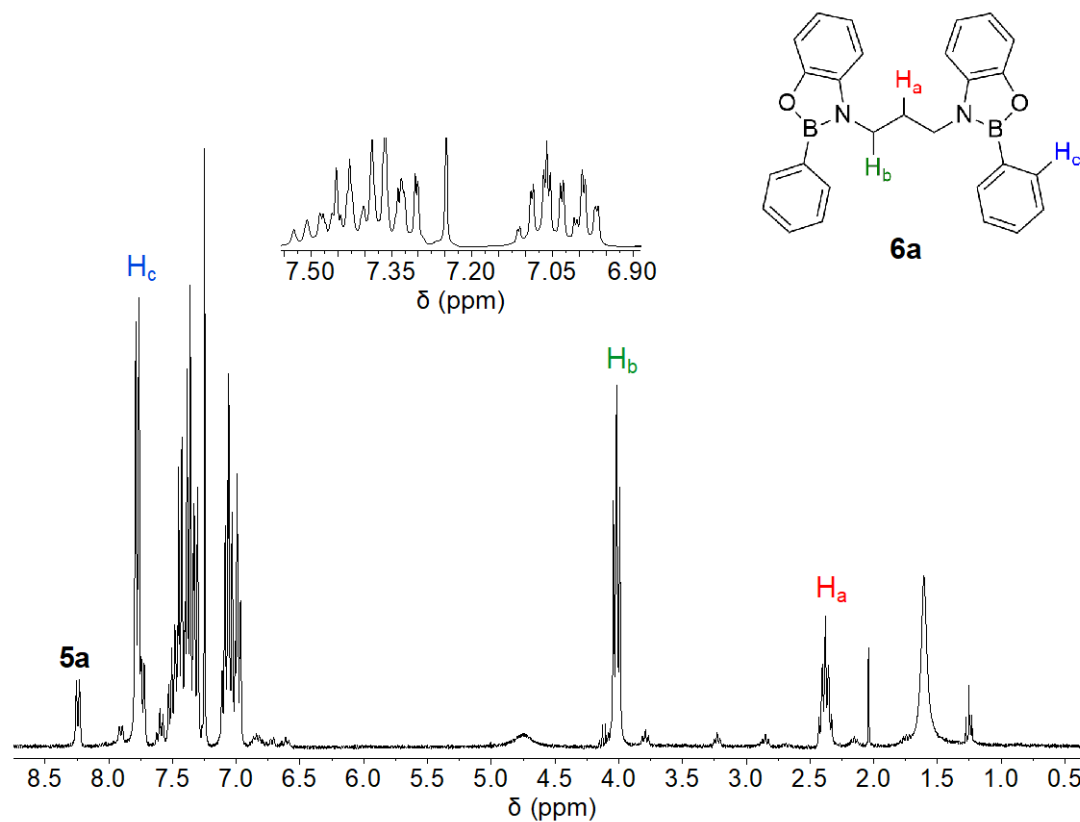


**Figure 27.**  $^1\text{H}$  NMR spectrum of the reaction mixture of propane-1,3-bis(aminophenol) (**3a**) and phenylboronic acid (**5**), in  $\text{CDCl}_3$ .

### Alkyl-Linked bis(benzoxazaborole) **6c**

Similar to the synthesis of propane-1,3-bis(benzoxazaborole) (**6a**) in  $\text{CDCl}_3$ , the synthesis of p-xylylene bis(benzoxazaborole) (**6c**) was attempted by mixing a 1:2 ratio of p-xylylene bis(aminophenol) (**3c**) and phenylboronic acid (**5**) in either  $\text{CDCl}_3$  or  $\text{THF-}d_8$  at room temperature or in toluene at  $60\text{ }^\circ\text{C}$  (Figure 28a-c).

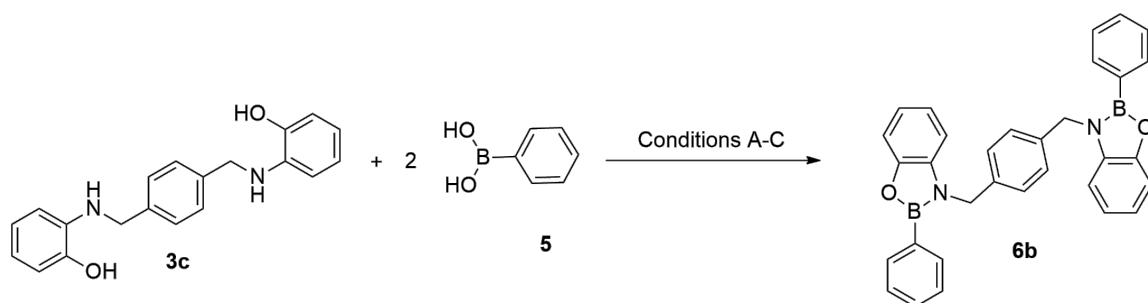


**Figure 28.** Synthesis of *p*-xylylene linked bis(benzoxazaborole) (**6c**) from the reaction between *p*-xylylene bis(aminophenol) (**3c**) and phenylboronic acid (**5**).; (a) CDCl<sub>3</sub> (25 °C) (b) THF-*d*<sub>8</sub> (25 °C) (c) toluene (60 °C).

The starting material, *p*-xylylene bis(aminophenol) (**3c**) did not completely dissolve in CDCl<sub>3</sub>. Furthermore, it remained undissolved even after the addition of phenylboronic acid (**5c**). The reaction mixture was analyzed by <sup>1</sup>H NMR, to monitor the progress of the reaction. The <sup>1</sup>H NMR spectrum showed evidence of product formation (new signals appeared at 5.2 and 7.0 ppm) within 30 min (Figure 29), along with the excess phenylboronic acid (**5**) and boroxine (**5a**) (Figure 26). However, the reaction did not go to completion and only reached 68% conversion even after the addition of molecular sieves (3Å). This may be mostly due to the low solubility of *p*-xylylene bis(aminophenol) (**3c**) in CDCl<sub>3</sub>. This result indicates CDCl<sub>3</sub> is not a good solvent to synthesize *p*-xylylene bis(benzoxazaborole) (**6c**), but it can be used to characterize the products as they have greater solubility in CDCl<sub>3</sub>.

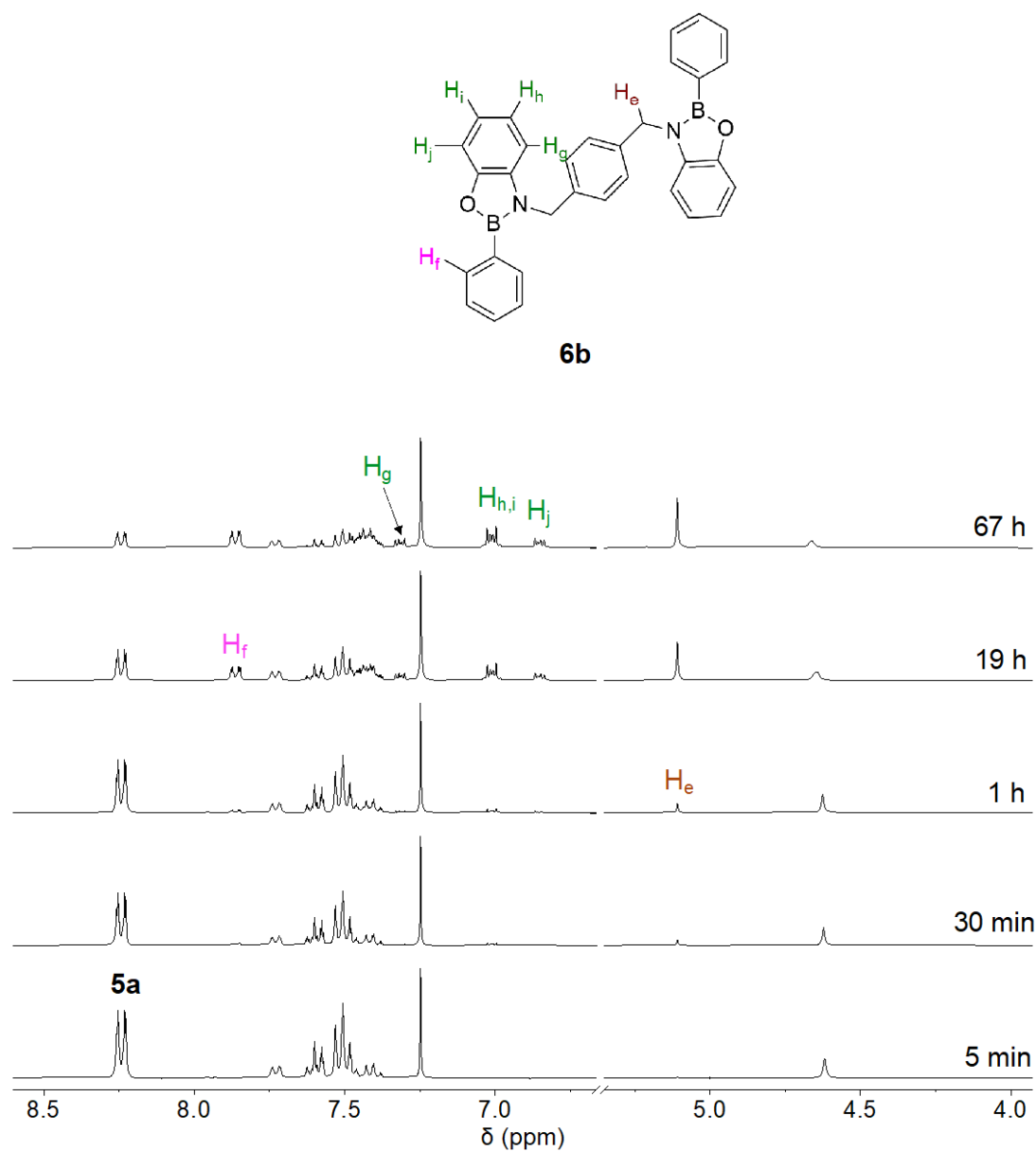


**Figure 29.** Stacked  $^1\text{H}$  NMR spectra of the reaction mixture of *p*-xylylene bis(aminophenol) (**3c**) and phenylboronic acid (**5**), in  $\text{CDCl}_3$ .

Next, the direct synthesis of bis(benzoxazaborole) **6c** was carried out in  $\text{THF-}d_8$  (Figure 27). First, *p*-xylylene bis(aminophenol) (**3c**) was dissolved in  $\text{THF-}d_8$ . Unlike in  $\text{CDCl}_3$ , bis(aminophenol) **3c** completely dissolved in  $\text{THF-}d_8$  at room temperature. After adding 2 equivalents of phenylboronic acid (**5**), 21% conversion was achieved within 5 minutes, which continued to increase up to 45% after 3 h. Three beads of molecular sieves

(3Å) were added to the mixture since there was not much change after that. After 25 hours, the conversion was about 76%, and molecular sieves were added a second time to achieve greater conversion.  $^1\text{H}$  NMR spectra were obtained over time to monitor the reaction progress (Figure 30). However, after 70 hours the maximum observed conversion was 89% (Figure 31).

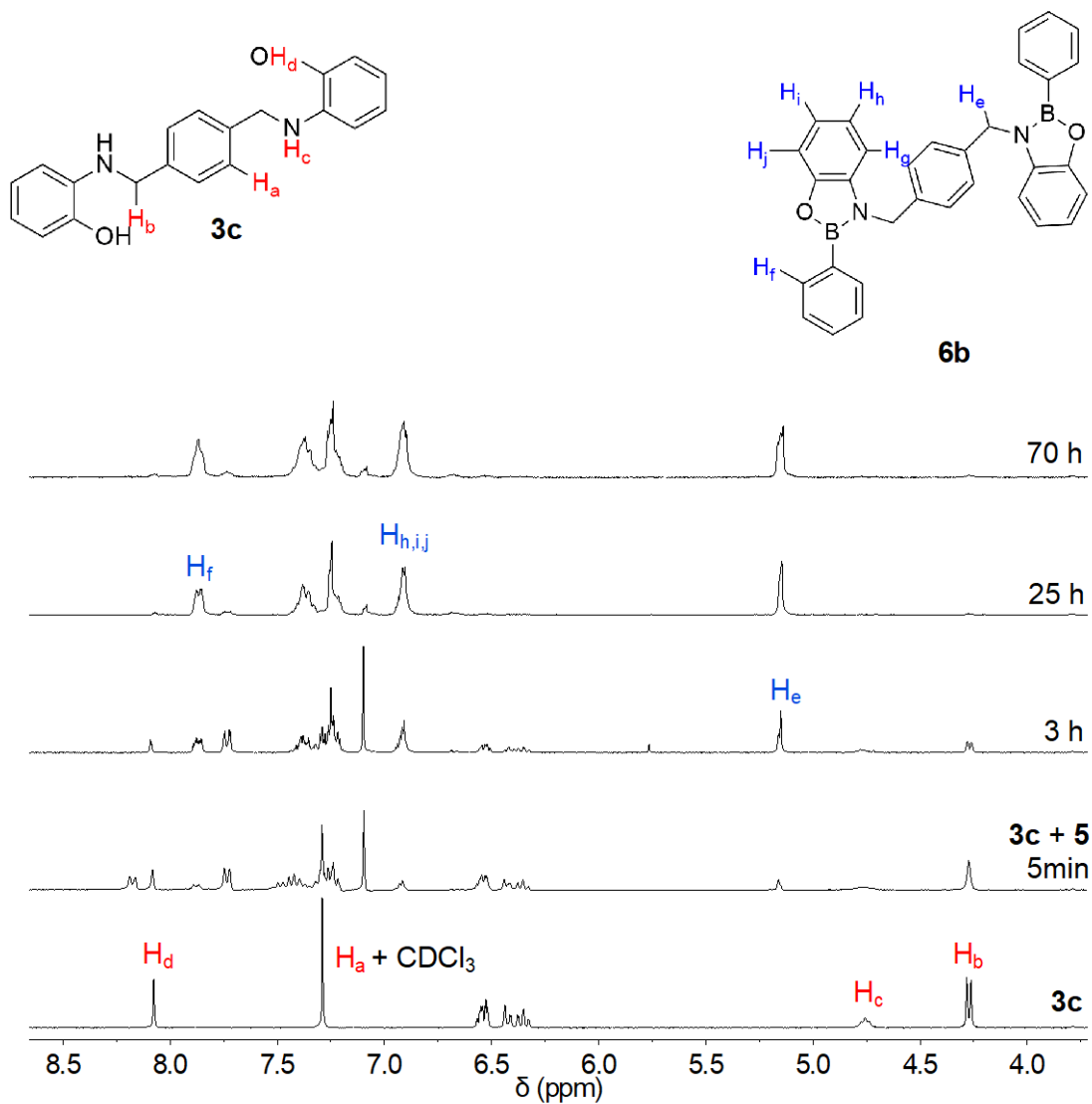


**Figure 30.** Stacked partial  $^1\text{H}$  NMR spectra for the synthesis of *p*-xylylene bis(benzoxazaborole) (**6c**). in  $\text{THF-d}_8$ .

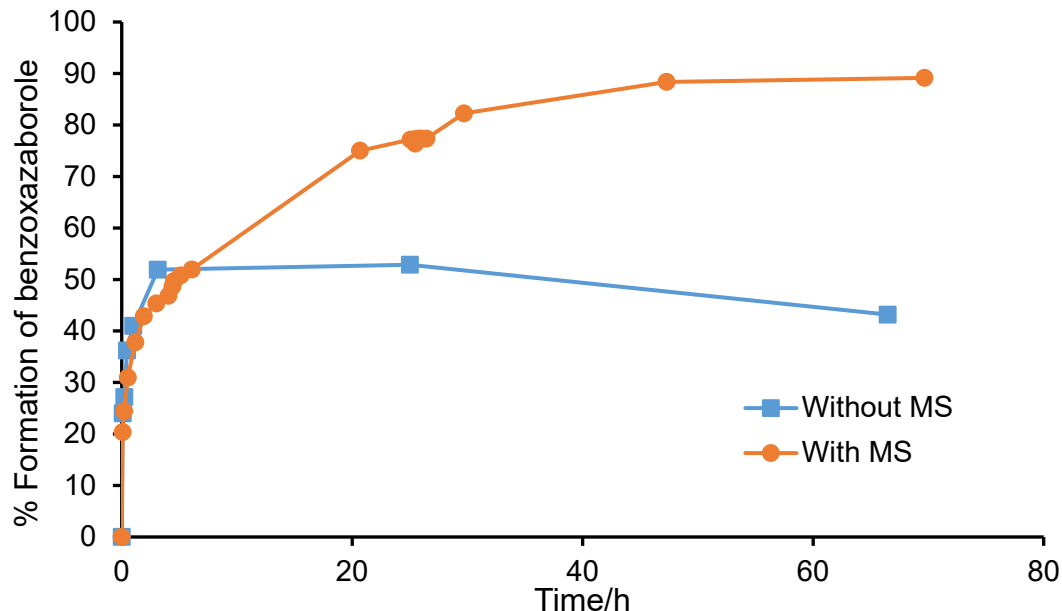


**Figure 31.** Percent formation of bis(benzoxazaborole) **6c** over time.

Based on the above observations, THF-*d*<sub>8</sub> is a good solvent for the characterization of the product as well as the starting materials as they are completely soluble at this concentration. Although the formation of **6c** was high (89%), it did not achieve full conversion. Also, the product **6c** is not likely to be stable in ambient atmosphere because the water can be absorbed by THF.

Next, similar to a synthetic method developed in our research group for benzodioxaborole and benzoxazaborole, the synthesis of p-xylylene bis(benzoxazaborole) (**6c**) was attempted by mixing a 1:2 ratio of p-xylylene bis(aminophenol) (**3c**) with phenylboronic acid (**5**) in toluene at 60 °C (Figure 27). The reaction was stirred at this temperature for 30 min and the solvent was removed under reduced pressure and the formation of the product was confirmed by <sup>1</sup>H NMR (Figure 32).

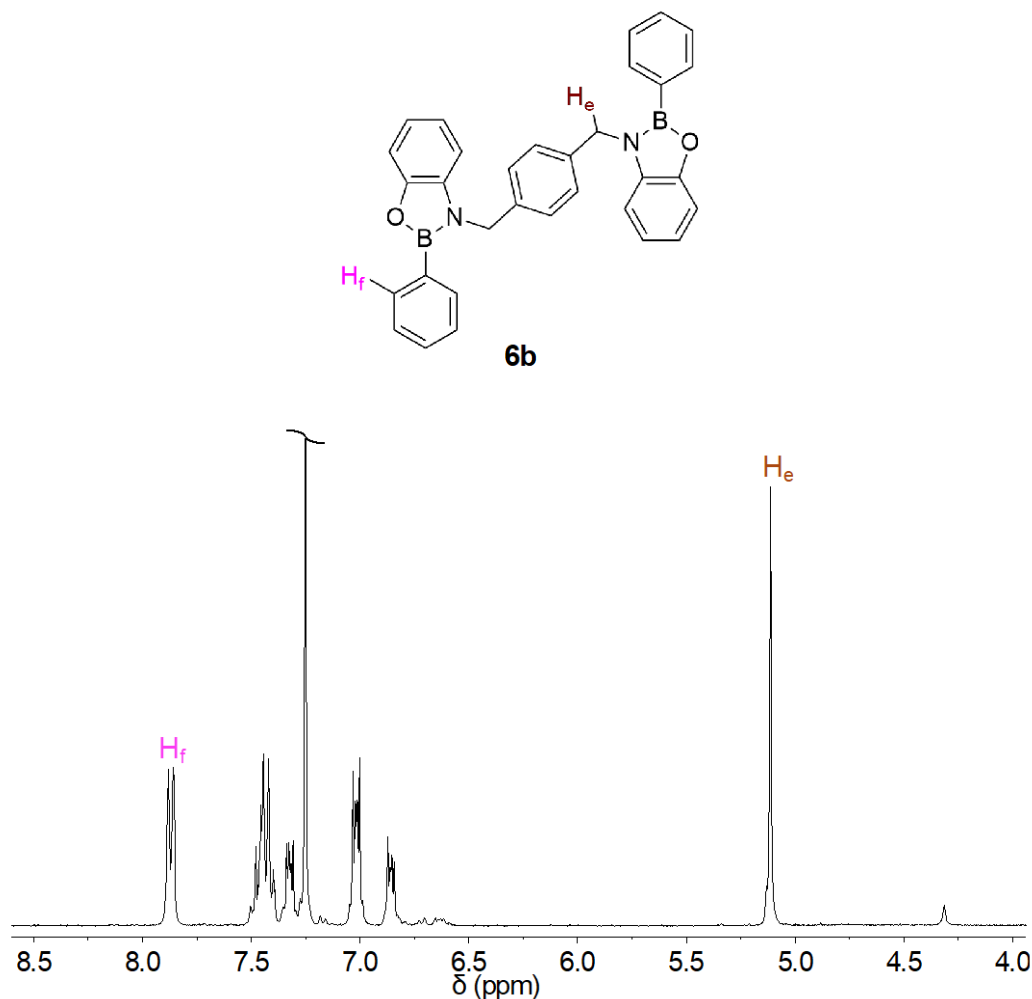


**Figure 32.** Partial  $^1H$  NMR spectrum of the product from the reaction between *p*-xylylene bis(aminophenol) (**3c**) and phenylboronic acid (**5**) from the solvent removal method.  $^1H$  NMR in  $CDCl_3$ .

The  $^1H$  NMR spectrum shows traces of bis(aminophenol) **3c** along with the product **6c**, and there is no trace of phenylboronic acid (**5**). These results indicate mixing in toluene at 60 °C may be a potential method for the synthesis of poly(benzoxazaborole)s compared to simple mixing in  $CDCl_3$  or  $THF-d_8$ .

### Poly(benzoxazaborole) **8**

With the promising initial results, we turned to the synthesis of poly or oligo(benzoxazaborole)s was attempted by mixing the starting materials, propane-1,3-

bis(aminophenol) (**3a**) and benzene diboronic acid (**7**), in a 1:1 ratio under various conditions (Figure 33).

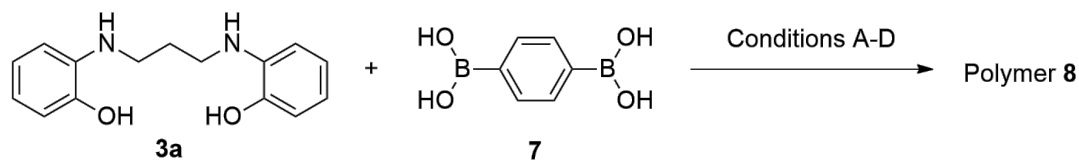


**Figure 33.** Attempted synthesis of poly(benzoxazaborole) **8** from the reaction between bis(aminophenol) **3a** and diboronic acid **7**. (a)  $\text{CDCl}_3$  (25 °C) (b)  $\text{DMSO-}d_6$  (25 °C) (c) ethyl acetate (25 °C) (d) reflux in toluene (110 °C).

Despite the low solubility of the bis(aminophenol) **3a**, the previous formation of bis(benzoxazaborole) **6a** was driven forward due to the dissolution of the product **6a** in  $\text{CDCl}_3$ . However, in the current case, there was no evidence of product formation when mixing bis(aminophenol) **3a** with benzene diboronic acid (**7**), as the  $^1\text{H}$  NMR did not show any signals except for the propane-1,3-bis(aminophenol) (**3a**). This is likely due to the lack of solubility of diboronic acid **7** in  $\text{CDCl}_3$ .

Next, the direct synthesis of oligo(benzoxazaborole) **8** from propane-1,3-bis(aminophenol) (**3a**) was attempted in  $\text{DMSO-}d_6$  at room temperature (Figure 33). Surprisingly, the mixing of the two reactants resulted in white precipitate within 10 minutes that continued to increase with time (Figure 34a & b).  $^1\text{H}$  NMR of the solid showed the appearance of new signals at the expected chemical shifts for the benzoxazaborole protons. These signals decreased over time (Figure 35), which may be due to the formation of insoluble oligomers and the growing insolubility as the polymer chain length increases. The increase in the intensity of the water signal is also further evidence that the amount of condensation increased over time and polymer growth was likely the reason. After 12 days a drop of water was added to the same NMR tube and after two days the amount of precipitate appeared to decrease (Figure 34 c&d). Additionally, the  $^1\text{H}$  NMR spectrum

displayed an increase of starting material bis(aminophenol) **3a**. This observation may be due to the hydrolysis of the product by the addition of water.

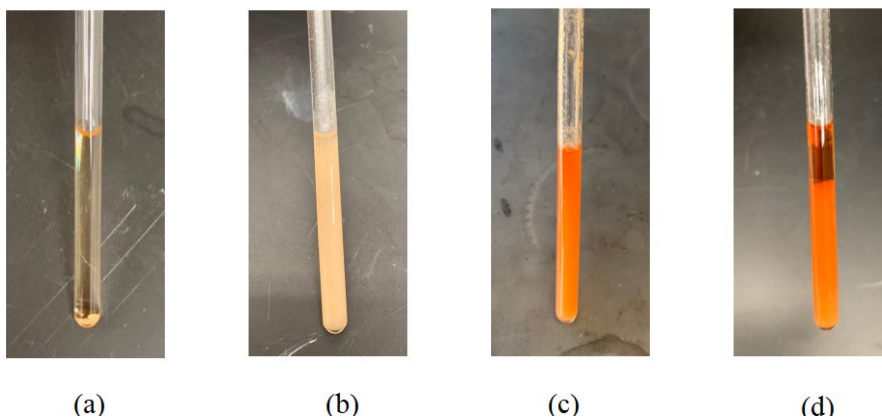


**Figure 34.** NMR tube containing 1:1 ratio of propane-1,3-bis(aminophenol) (**3a**) and benzene diboronic acid (**7**). in DMSO- $d_6$ ; (a) right after mixing (b) 10 min (c) 12 days (d) 14 days and after adding water.

Next, starting materials **3a** and **7** were mixed in a 1:1 ratio in ethyl acetate (EtOAc) and stirred for 30 minutes. Eventually, the starting materials dissolved, and subsequently, a white solid appeared. Attempts were made to analyze the product by  $^1\text{H}$  NMR but it did not dissolve in  $\text{CDCl}_3$ .

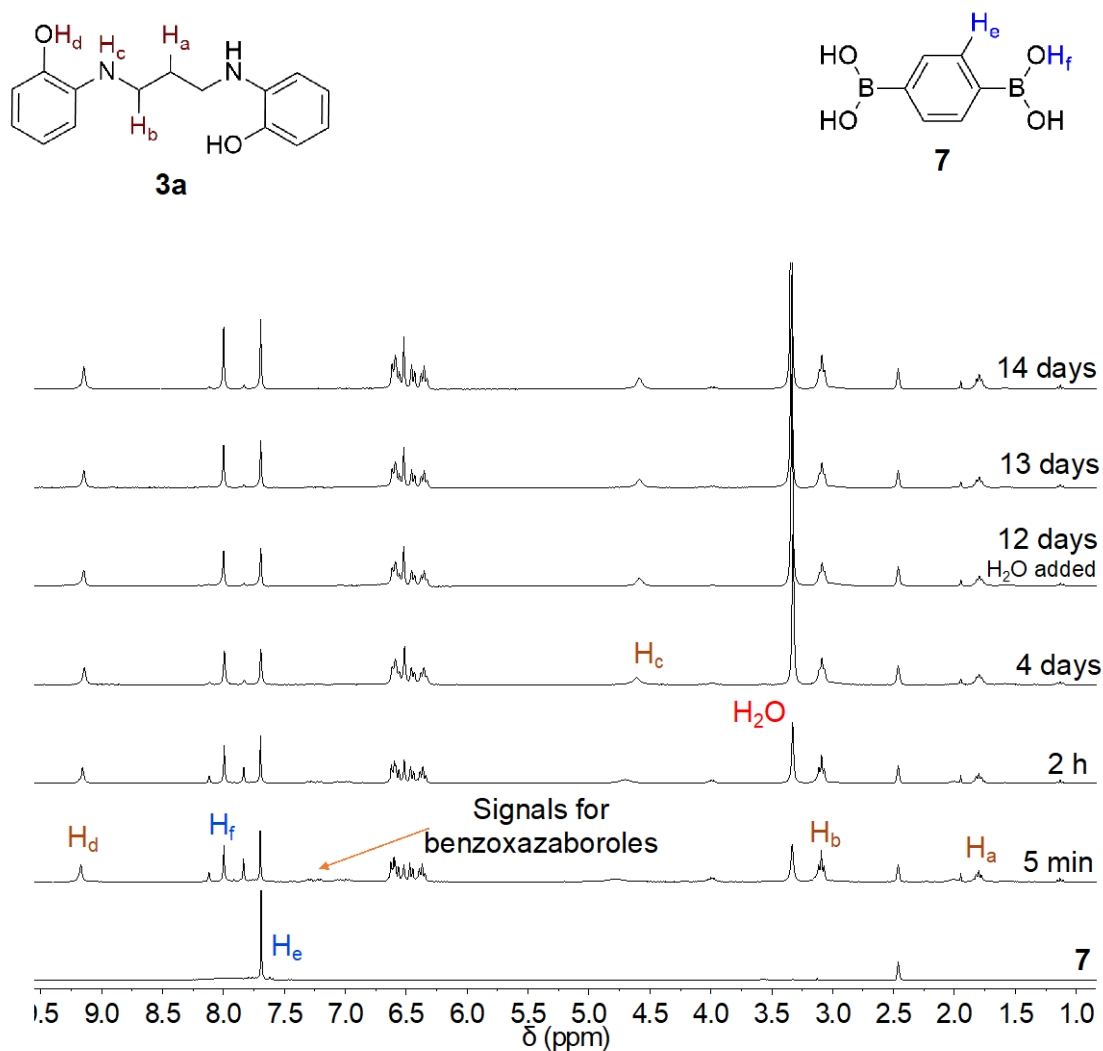


**Figure 35.** Stacked  $^1\text{H}$  NMR spectra for the synthesis of poly(benzoxazaborole) in  $\text{DMSO-}d_6$ .

Next, the condensation reaction was carried out using previously reported conditions.<sup>41,42</sup> Monomers **3a** and **7** were mixed in ethanol and toluene and refluxed overnight (Figure 33). Upon cooling, a colorless crystalline solid was obtained (Figure 36). Characterization of poly(benzoxazaborole) **8** using  $^1\text{H}$  NMR and  $^{13}\text{C}$  NMR was not possible due to poor solubility of poly(benzoxazaborole) in common organic solvents such as chloroform, dimethyl sulfoxide, tetrahydrofuran, acetone, dichloromethane, ethyl acetate, *N,N*-dimethylformamide, ethanol, acetonitrile, and water.



**Figure 36.** The crystalline solid obtained from the reaction of propane-1,3-bis(aminophenol) (**3a**) and benzene diboronic acid (**7**).

### Poly(benzoxazaborole) **9**

Similar to the synthesis of propane-1,3-poly(benzoxazaborole) (**8**) the synthesis of poly(benzoxazaborole) **9** was carried out by mixing starting materials, *p*-xylylene poly(benzoxazaborole) (**3c**), and benzene diboronic acid (**7**) in a 1:1 ratio under various conditions (Figure 36).

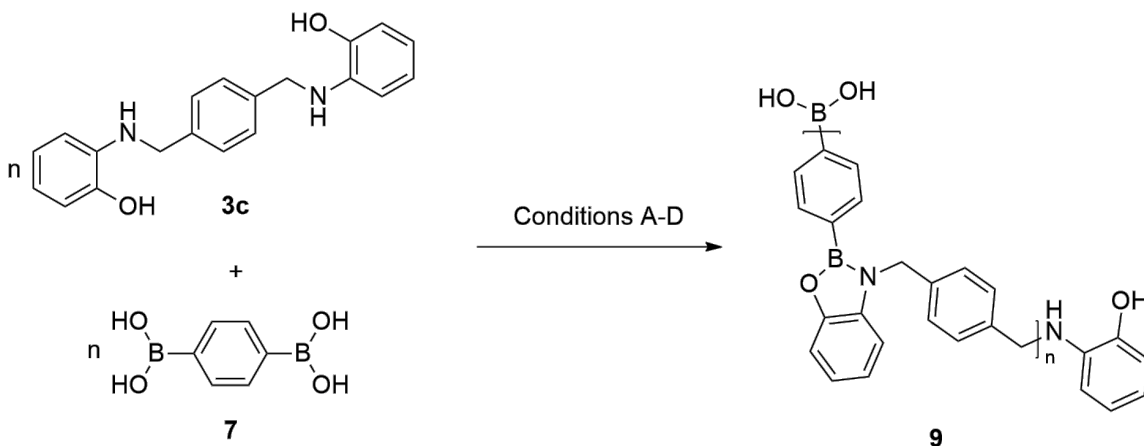


**Figure 37.** Synthesis of *p*-xylylene based poly(benzoxazaborole) (**9**) from the reaction between *p*-xylylene bis(aminophenol) (**3c**) and benzene diboronic acid (**7**). (a) DMSO- $d_6$  (25 °C) (b) THF- $d_8$  (25 °C) (c) toluene (60 °C) (d) reflux in toluene (110 °C).

The formation of poly(benzoxazaborole) **9** was not attempted in  $\text{CDCl}_3$  due to poor solubility of both starting materials, **3c** and **7**. In DMSO- $d_6$ , there was no evidence of

precipitation from the reaction as in the previous experiment involving **3a**. However, the  $^1\text{H}$  NMR showed evidence of benzoxazaborole formation immediately after mixing the starting materials, which did not increase significantly over time (Figure 37).

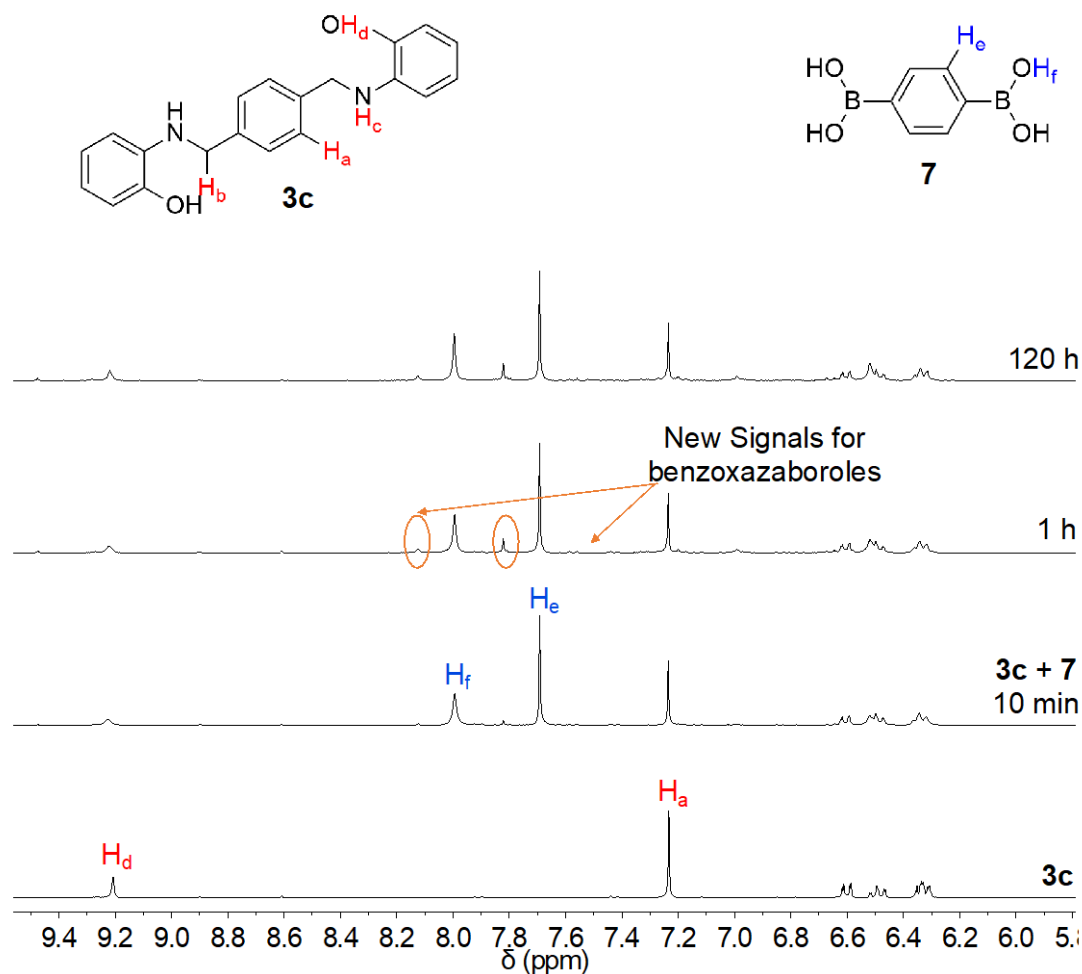


**Figure 38.** Stacked  $^1\text{H}$  NMR spectra for the synthesis of poly(benzoxazaborole) **9** in  $\text{DMSO}-d_6$ .

When using  $\text{THF}-d_8$  as the reaction solvent, benzoxazaborole formation was also observed according to  $^1\text{H}$  NMR analysis (Figure 38). However, only 50% of the starting materials were consumed. These incomplete reactions may be due to the presence and miscibility of water in both  $\text{DMSO}-d_6$  and  $\text{THF}-d_8$ .

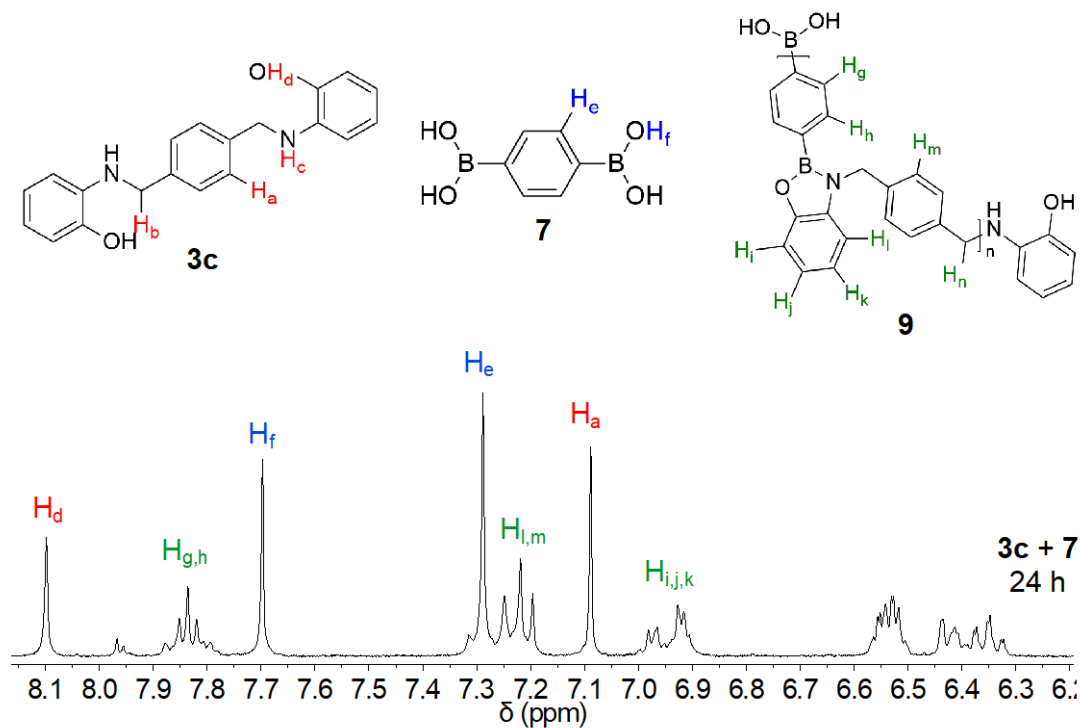


**Figure 39.** Partial  $^1\text{H}$  NMR spectrum for the synthesis of poly(benzoxazaborole) **9** in  $\text{THF-}d_8$ .

With evidence of reactivity in both  $\text{DMSO-}d_6$  and  $\text{THF-}d_8$ , the synthesis of poly(benzoxazaborole) was attempted in toluene. When heating the reaction mixture at  $60^\circ\text{C}$  a white precipitate formed, which is sparingly soluble in  $\text{CDCl}_3$ . The  $^1\text{H}$  NMR spectrum had new signals at the chemical shifts that would be expected for benzoxazaborole formation (Figure 39) but most of the sample remained undissolved. This is an indication that the sample may contain more than one product, and that some products are soluble in  $\text{CDCl}_3$ .

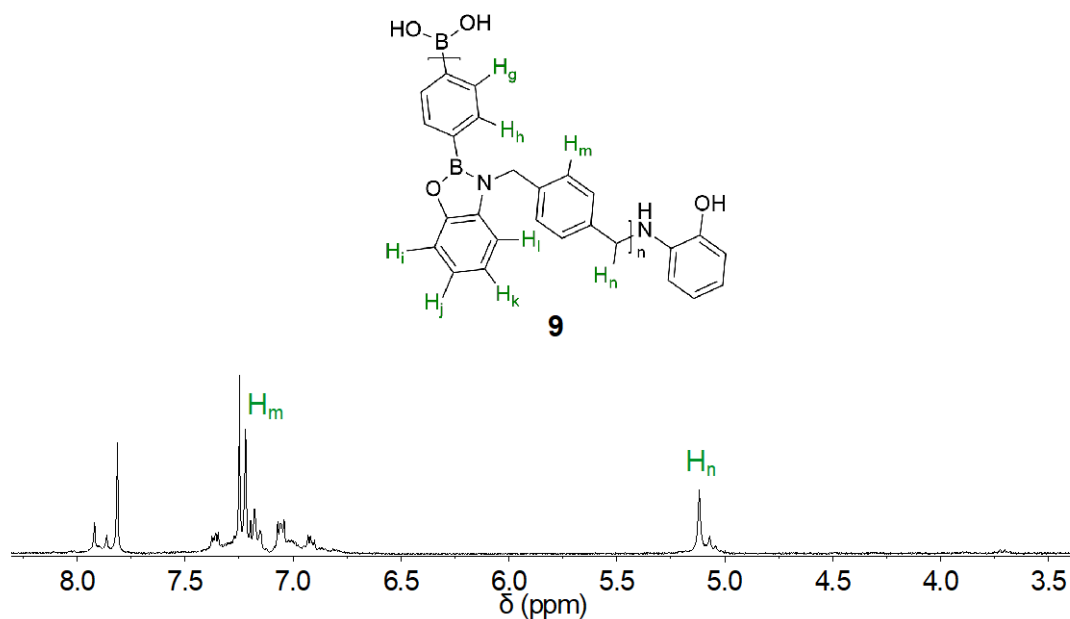


**Figure 40.** Partial  $^1\text{H}$  NMR spectrum for the synthesis of poly(benzoxazaborole) **9**. in toluene at 60 °C.

Next, the starting materials **3c** and **7** were mixed in a 1:1 ratio in EtOH and toluene and refluxed overnight to obtain a white crystalline solid (Figure 40). In this case, when attempting NMR analysis of the solid in  $\text{CDCl}_3$  no signals were observed.  $^1\text{H}$  NMR and  $^{13}\text{C}$  NMR analysis were not successful as no signals were observed, likely due to poor solubility of poly(benzoxazaborole), which was also insoluble in other common organic solvents such as  $\text{CDCl}_3$ ,  $\text{DMSO-}d_6$ ,  $\text{THF-}d_8$ , acetone, DCM, benzene, hexane, acetonitrile, and in DMF.

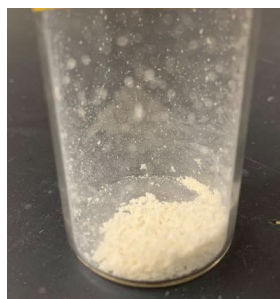


**Figure 41.** White crystals from the reaction of *p*-xylylene bis(aminophenol) (**3c**) and benzene diboronic acid (**7**).

Two drops of H<sub>2</sub>O were added to the NMR tube, which contained polymer **9** in DMSO-*d*<sub>6</sub> and it was analyzed by <sup>1</sup>H NMR over time. The spectrum showed signals related to the starting materials. This indicates hydrolysis of polymer **9** into starting materials due to the addition of water (Figure 41) and that polymer **9** may possess dynamic covalent nature and can be converted back to starting monomers under mild conditions.

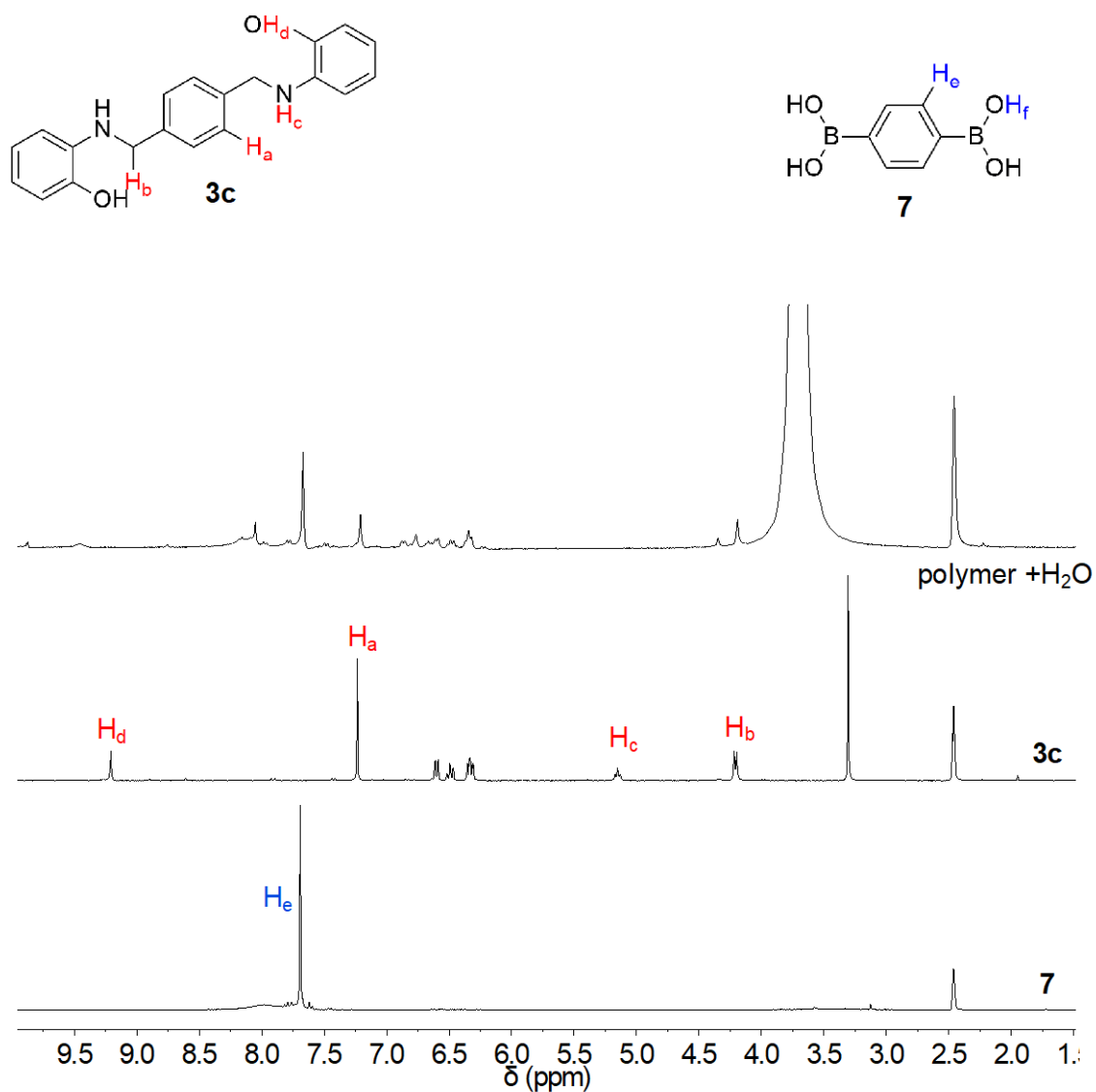


**Figure 42.** Partial stacked <sup>1</sup>H NMR spectra for the hydrolysis of poly(benzoxazaborole) **9** with the addition of H<sub>2</sub>O in DMSO-*d*<sub>6</sub>.

**Melting Point Analysis of Benzoxazaboroles.** During the melting point experiment for polymer **8**, the bis(aminophenol) **3a** decomposed at 157-159 °C by turning dark brown and the benzene diboronic acid (**7**) did not melt below 400 °C. The isolated polymer material decomposed at 325-326 °C whereas a 1:1 mixture of two starting materials only partially decomposed at 276-279 °C and the rest did not melt until 400 °C (Table 1). The results from this melting point analysis reveal that the isolated product from the reaction is not simply a mixture of starting materials and it is further evidence of polymerization.

**Table 1.** *Melting point data for 3a, 7, 3a+7 and polymer 8*

Compound	Melting point (°C)
<b>3a</b>	157-159 (dec.)
<b>7</b>	>400
1:1 mixture of <b>3a</b> + <b>7</b>	276-279 (partial) >400
polymer product	325-326 (dec.)

During the melting point experiment for polymer **9**, the bis(aminophenol) **3c** decomposed completely at 205-206 °C and the benzene diboronic acid (**7**) did not melt below 400 °C. The isolated polymer material decomposed at 364-366 °C whereas a 1:1 mixture of two starting materials only partially decomposed at 238-240 °C and the rest did not melt until 400 °C (Table 2). The results from this melting point analysis reveal that the isolated product from the reaction is not simply a mixture of starting materials and it is further evidence that polymerization did occur in the reaction.

**Table 2.** *Melting point data for 3c, 7, 3c+7 and polymer 9*

Compound	Melting point (°C)
<b>3c</b>	205-206 (dec.)
<b>7</b>	>400
1:1 mixture of <b>3c+7</b>	238-240 (partial)
	>400
polymer product	364-366 (dec.)

**FTIR Analysis of Benzoxazaboroles.** FTIR spectroscopic analysis for the characterization of benzoxazaboroles can sometimes be misleading as they share the same functionality as seen in the reactants. However, the most obvious spectral change in the formation of benzoxazaboroles is the disappearance of the broad peak in the range of 3500-3100  $\text{cm}^{-1}$ . This indicates the disappearance of OH and NH functionalities present in the starting materials. However, the linear oligomeric materials may also contain terminal NH and OH moieties, but these signals would not be expected if the oligomers were significantly long or cyclic. The analysis of bis(benzoxazaboroles)s **6a**, **6c**, polymers **8**, **9**, aminophenols **3a**, **3c**, phenylboronic acid (**5**), and benzene diboronic acid (**7**) was carried out (Table 3).

The IR spectra related to the bis(benzoxazaborole)s **6a** and **6c** do not show the corresponding peaks for the starting materials. This supports the consumption of the starting materials and the **6a** and **6b** do not contain mono(benzoxazaboroles)s (Figure 43, Figure 44). (See Appendix B for the complete spectra)

Polymers **8** and **9** do not show the signals for OH and NH moieties. The absence of the corresponding signals for the starting materials supports the consumption of the starting materials and a high degree of polymerization for both polymers **8** and **9** (Figure 45 and Figure 46).

**Table 3.** FTIR data for aminophenols **3a**, **3c**, phenylboronic acid (**5**), benzene diboronic acid (**7**)

Compound	Functional group	Stretching frequency (cm <sup>-1</sup> )
<b>3a</b>	OH	3213 (br)*
	NH	3315
<b>3c</b>	OH	3303 (br)
	NH	3220
<b>5</b>	OH	3236 (br)
<b>7</b>	OH	3290 (br)

\*br-broad

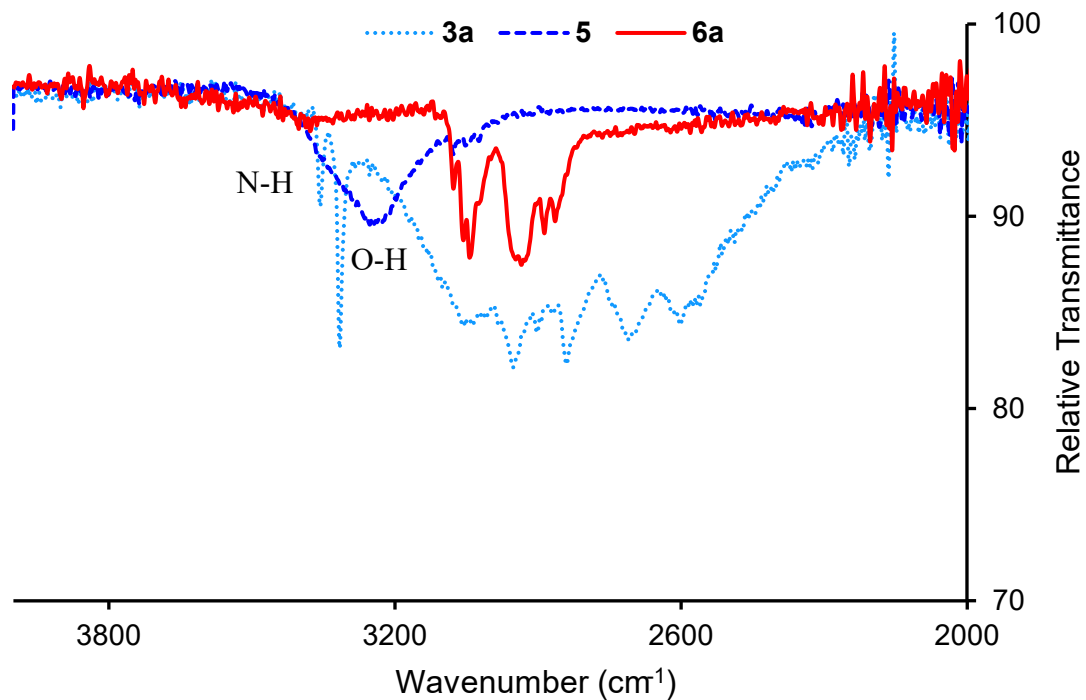


**Figure 43.** FTIR spectra of propane-1,3-bis(aminophenol) (**3a**), phenylboronic acid (**5**), and propane-1,3-bis(benzoxazaborole) (**6a**).

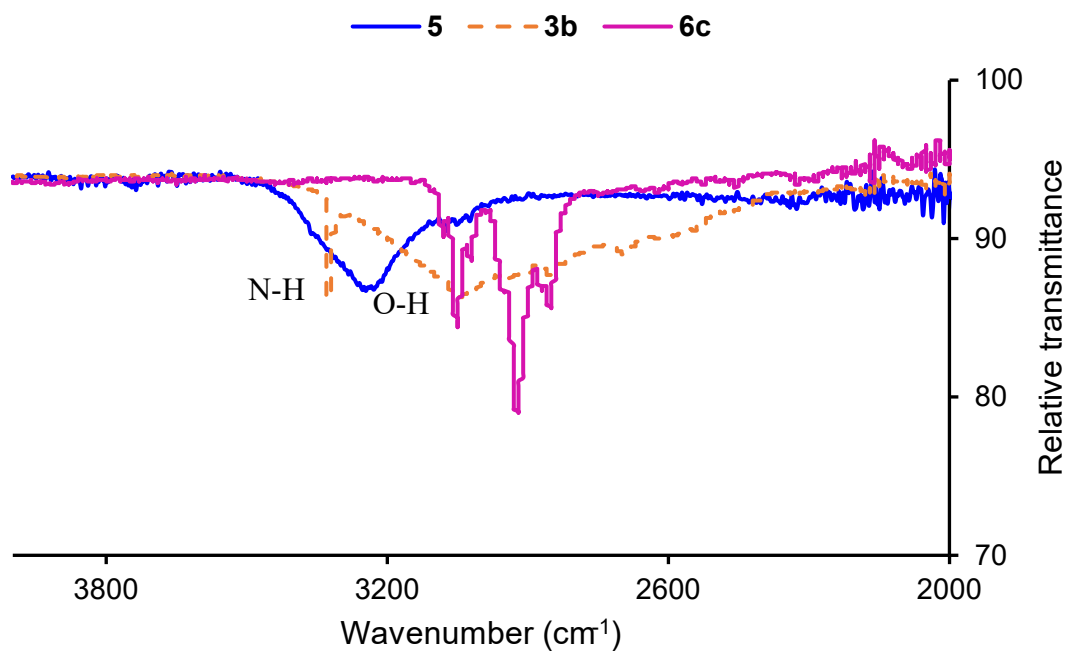


**Figure 44.** FTIR spectra of *p*-xylylene bis(aminophenol) (**3c**), phenylboronic acid (**5**), and *p*-xylylene bis(benzoxazaborole) (**6b**).

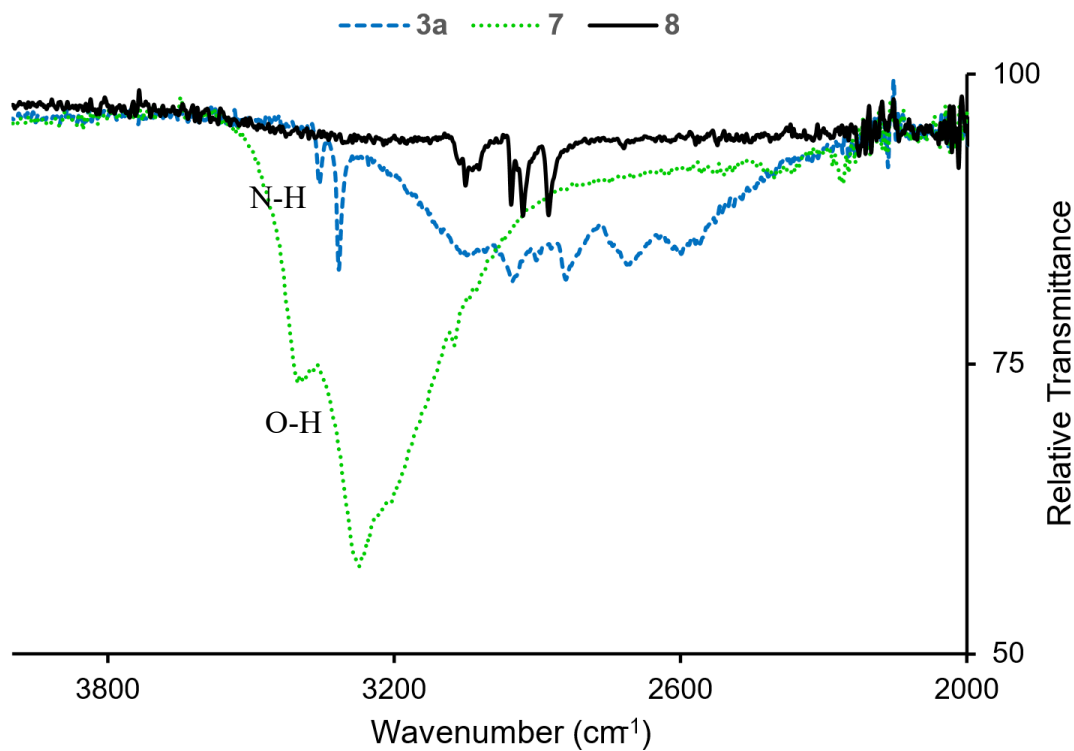


**Figure 45.** FTIR spectra of propane-1,3-bis(aminophenol) (**3a**), benzene diboronic acid (**7**), and propane-1,3-poly(benzoxazaborole) (**8**).

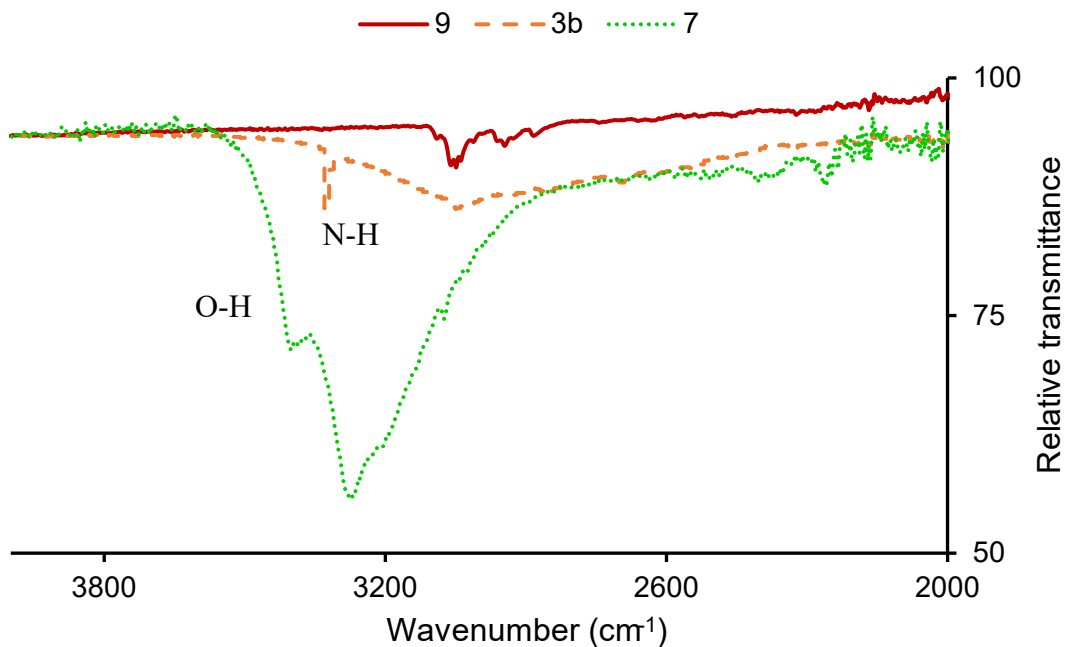


**Figure 46.** FTIR spectra of *p*-xylylene bis(aminophenol) (**3c**), benzene diboronic acid (**7**), and *p*-xylylene poly(benzoxazaborole) (**9**).

## Computational Studies on the Synthesis and Ring–Chain Equilibrium of Poly(benzoxazaborole)s

Recently, Northrop and Drogkaris investigated the thermodynamics of several conjugated boronate esters using computational chemistry.<sup>47</sup> Previously, our research group has investigated the thermodynamics of several diazaboroles in different solvents and the thermodynamics of *N*-alkyl benzoxazaboroles as well as bis(benzoxazaborole)s in the gas phase.<sup>41,48</sup> The computational calculations for thermodynamics and ring-chain equilibrium of alkyl-linked poly(benzoxazaborole)s in the gas phase have not been reported yet.

This study focuses on the stability of cyclic and acyclic oligo(benzoxazaborole)s, which can result from the reaction of bis(aminophenol)s **3a** and **3c** with diboronic acid **7**. The optimal geometries of the molecules were obtained utilizing the molecular mechanics/UFF method. Then, the resulting optimized structures were optimized again with semi-empirical level and PM3 function to obtain geometries with the lowest energy. Finally, the optimized geometries were subjected to geometry optimization using computationally cheap, Hartree-Fock (HF) level with minimal basis set (3-21 G) to obtain more accurate geometry. The frequencies were calculated using the same level of theory. The Gibbs free energies of formation ( $\Delta G_{\text{formation}}$ ) of possible cyclic and acyclic oligo(benzoxazaborole)s (Figure 47 & Figure 48) were calculated in the gas phase at room temperature (298 K) using the equation  $\Delta G_{\text{formation}} = E_{\text{products}} - E_{\text{reactants}}$  (Table 4 & Table 5).

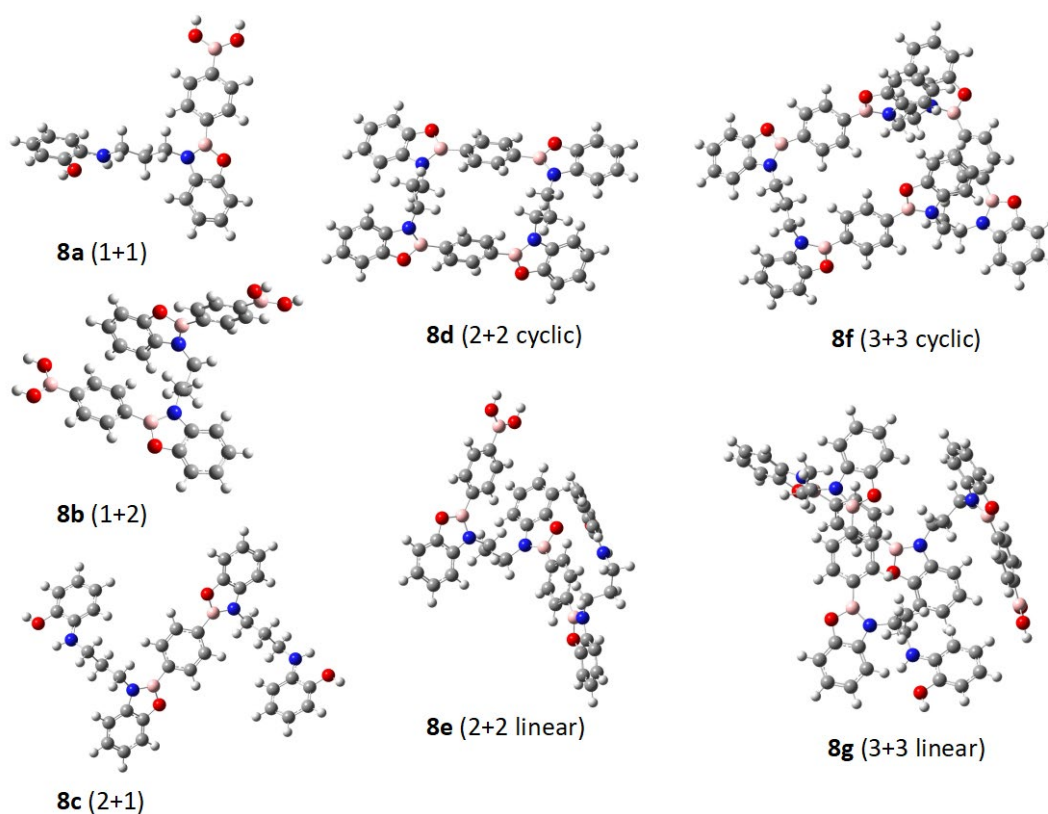


**Figure 47.** The optimized structures of linear and cyclic oligo(benzoxazaborole)s **8**.

**Table 4.** Computational results for oligo(benzoxazaborole)s **8a-g**.

	$E_{\text{products}}$ (Hartrees)		$E_{\text{reactants}}$ (Hartrees)		$\Delta G_{\text{formation}}$	
	Benzoxazaborole	H <sub>2</sub> O	Bis(aminophenol)	BDBA	(Hartrees)	(kJ/mol)
<b>8a</b>	-1258.611	-151.164	-832.170	-577.593	-0.012	-31.5
<b>8b</b>	-1685.045	-302.327	-832.170	-1155.185	-0.017	-44.4
<b>8c</b>	-1939.599	-302.327	-1664.339	-577.593	0.005	13.9
<b>8d</b>	-2214.855	-604.655	-1664.339	-1155.185	0.015	39.7
<b>8e</b>	-2366.036	-453.491	-1664.339	-1155.185	-0.003	-7.0
<b>8f</b>	-3322.269	-906.982	-2496.509	-1732.778	0.036	95.2
<b>8g</b>	-3473.451	-755.818	-2496.509	-1732.778	0.018	47.8

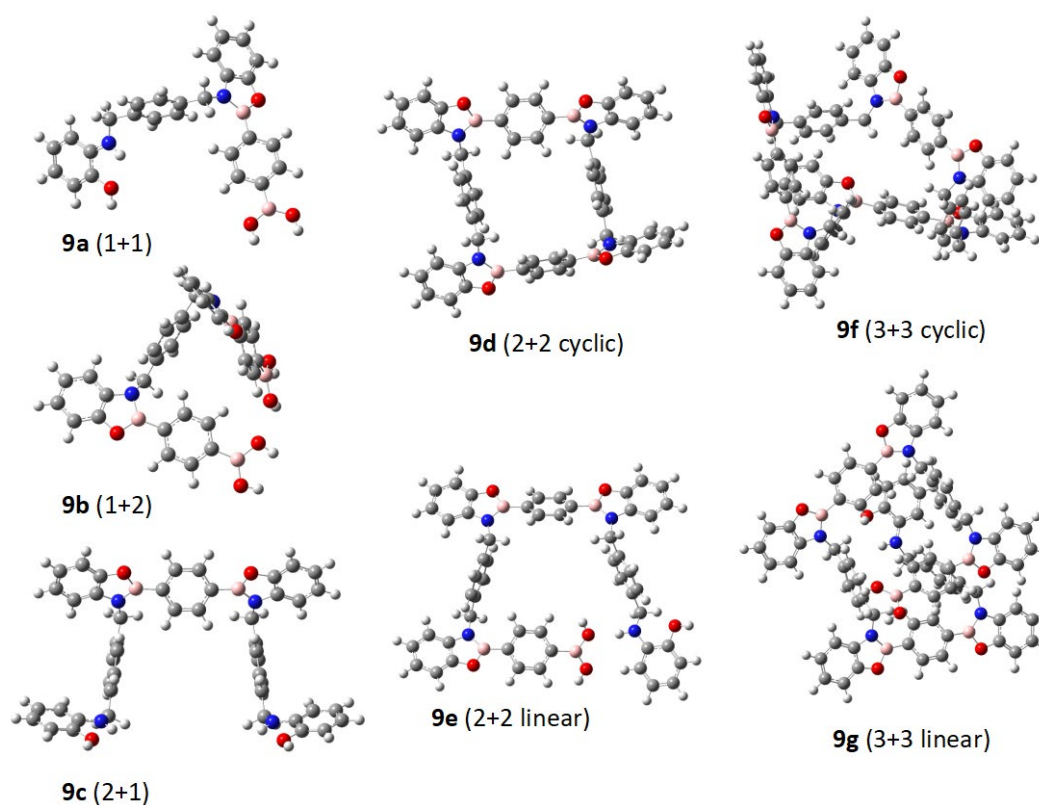


**Figure 48.** The optimized structures of linear and cyclic oligo(benzoxazaborole)s **9**.

**Table 5.** Computational results for oligo(benzoxazaborole)s **9a-g**.

	Products (Hartrees)		Reactants (Hartrees)		$\Delta G$ (P-R) (Hartrees)	$\Delta G$ (kJ/mol)
	Benzoxazaborole	H <sub>2</sub> O	Bis(aminophenol)	BDBA		
<b>9a</b>	-1448.007	-151.164	-1021.565	-577.593	-0.013	-34.6
<b>9b</b>	-1874.439	-302.327	-1021.565	-1155.185	-0.016	-41.6
<b>9c</b>	-2318.396	-302.327	-2043.130	-577.593	-0.001	-1.6
<b>9d</b>	-2593.647	-604.655	-2043.130	-1155.185	0.014	37.0
<b>9e</b>	-2744.820	-453.491	-2043.130	-1155.185	0.004	10.4
<b>9f</b>	-3890.465	-906.982	-3064.695	-1732.778	0.026	69.6
<b>9g</b>	-4041.649	-755.818	-3064.695	-1732.778	0.006	16.2

Next, the  $\Delta G_{\text{formation}}$  per oxazaborole ring was calculated by dividing the  $\Delta G_{\text{formation}}$  for the reaction by the number of borole rings in that particular structure to compare the relative stability of the oligo(benzoxazaborole)s (Table 6). According to the data, when comparing energies for structures, **8d** to **8e** and **8f** to **8g** in both cases, structures **8d** and **8f** show relatively higher energies than the structures **8e** and **8g**, respectively. Structures **8e** and **8g** are acyclic oligomers, and **8d** and **8f** are cyclic, which might cause them to have ring strain. From this result, it appears that the linear benzoxazaboroles are calculated to be more stable compared to cyclic structures in the gas phase, although the difference in energy is small.

**Table 6.**  $\Delta G$  calculations per benzoxazaborole ring for oligo(benzoxazaboroles).

	<i>Propyl linker</i>		<i>P-xylylene linker</i>	
	$\Delta G$ (P-R) (kJ/mol)	$\Delta G$ per benzoxazaborole ring (kJ/mol)		$\Delta G$ per benzoxazaborole ring (kJ/mol)
<b>8a</b>	-31.532	-31.532	<b>9a</b>	-34.554
<b>8b</b>	-44.439	-22.220	<b>9b</b>	-41.559
<b>8c</b>	13.886	6.943	<b>9c</b>	-1.562
<b>8d</b>	39.656	9.914	<b>9d</b>	36.972
<b>8e</b>	-7.039	-2.346	<b>9e</b>	10.384
<b>8f</b>	95.245	15.874	<b>9f</b>	69.576
<b>8g</b>	47.810	9.562	<b>9g</b>	16.244

Further analysis of the data indicates that the  $\Delta G_{\text{formation}}$  per benzoxazaborole ring varies depending on the type of linkage. We have named these linkages P and B to represent

when two benzoxazaborole rings are linked through the *propyl*-linked bis(aminophenol) and the *benzene* diboronic acid units, respectively (see structures **8b** and **8c** for example). One would expect that if there was no dependence on the linkage, that the 1+2 (**8b**) and 2+1 (**8c**) would simply have double the  $\Delta G_{formation}$  as the simple benzoxazaborole 1+1 (**8a**) system. However, when there is a P linkage (**8b**), the  $\Delta G_{formation}$  was not the predicted -63.1 kJ/mol but it was found to be -44.4 kJ/mol (Table 7). The difference between the calculated and predicted values for the 1+2 structure is 18.7 kJ/mol and when there is a B (i.e., **8c**) linkage the difference between the calculated and predicted is 77.0 kJ/mol. This may be mainly due to the difference in the connectivity of the benzoxazaborole rings within the structure. Structure **8b** has two isolated oxazaborole rings connected by a propyl chain (P linkage) in contrast **8c** has a bis(benzoxazaborole) that is connected to the 1,4 positions on the benzene ring of benzene diboronic acid (B linkage). The bis(benzoxazaborole) participating in the latter system may be less stable due to the conjugation.

**Table 7.** Predicted  $\Delta G_{formation}$  of benzoxazaboroles for oligo(benzoxazaborole)s **8a-g**.

	$\Delta G$ (kJ/mol)		Difference of $\Delta G$ (kJ/mol)		
	Predicted (based on # BOAB rings)	Actual calculated (P-R)	Difference	Predicted (based on # and type of linkage)*	Type of linkage**
<b>8a</b>	-31.5	-31.5	0.0	0.0	None
<b>8b</b>	-63.0	-44.4	18.6	18.6	1P
<b>8c</b>	-63.0	13.9	76.9	76.9	1B
<b>8d</b>	-126.0	39.7	165.7	190.8	2P & 2B
<b>8e</b>	-94.5	-7.0	87.5	95.4	1P & 1B

(continued)

<b>8f</b>	-189.0	95.2	284.2	286.2	3P & 3B
<b>8g</b>	-157.5	47.8	205.3	190.8	2P & 2B

\*Determined by taking the values for **8b** and **8c** and multiplying them by the number of linkages (P and B). See experimental section for details.

\*\*P - benzoxazaborole is linked through the bis(aminophenol) and B - benzoxazaborole is linked through the benzene diboronic acid.

Structure **8d** (2+2 cyclic) has two P linkages and two B linkages, and the difference in energy is 165.7 kJ/mol, which is closer to the predicted 190.8 kJ/mol. For structure **8e** (2+2 linear) the difference is 87.5 kJ/mol and it is closer to the 95.4 kJ/mol predicted energy. The predicted difference for structure **8f** (3+3 cyclic) is 286.2 kJ/mol as it has 3 P linkages and 3 B linkages. It exhibits 284.2 kJ/mol difference in energy, which is very close to the predicted value based on type of linkage. The structure **8g** (3+3 linear) has two P linkages and two B linkages similar to the **8d** (2+2 cyclic). The actual difference in energy is 205.3 kJ/mol at it is closer to the predicted 190.8 kJ/mol.

Similar to previous experiments, the values for  $\Delta G_{formation}$  of benzoxazaboroles were analyzed when the linker on the bis(aminophenol) is p-xylylene (Table 8). However, when the linkage is P (**9b**), the difference of  $\Delta G_{formation}$  between the calculated and predicted values is 27.5 kJ/mol and when there is a B linkage (**9c**) the difference is 67.5 kJ/mol. The predicted difference based on type of linkage is 190 kJ/mol for both **9d** (2+2 cyclic) and **9g** (3+3 linear) structures, which consist of two P linkages and two B linkages. The actual differences are closer to the predicted in both cases that are 175.2 kJ/mol for **9d** (2+2 cyclic) whereas it is 189.0 kJ/mol for **9g** (3+3 linear). The actual difference is 114.0 kJ/mol and it is closer to the 95.1 kJ/mol for structure **9e** (2+2 linear). This is half of the predicted value for corresponding cyclic structure as it has only one linkage of each type. The

predicted difference for **9f** (3+3 cyclic) structure is 285.3 kJ/mol as it has 3 P linkages and 3 B linkages. It exhibits 276.9 kJ/mol difference in energy, which is close to the predicted value based on the type of linkage.

**Table 8.** Predicted  $\Delta G_{\text{formation}}$  of benzoxazaboroles for oligo(benzoxazaborole)s **9a-g**.

	$\Delta G$ (kJ/mol)		Difference of $\Delta G$ (kJ/mol)		
	Predicted (based on # BOAB)	Actual (P-R)	Actual	Predicted (based on the type of link)	Type of linkage
<b>9a</b>	-34.6	-34.6	0.0	0.0	None
<b>9b</b>	-69.1	-41.6	27.5	27.5	1P
<b>9c</b>	-69.1	-1.6	67.5	67.5	1B
<b>9d</b>	-138.2	37.0	175.2	190.2	2P and 2B
<b>9e</b>	-103.7	10.4	114.0	95.1	1P and 1B
<b>9f</b>	-207.3	69.6	276.9	285.3	3P and 3B
<b>9g</b>	-172.8	16.2	189.0	190.2	2P and 2B

\*P benzoxazaborole is linked through the bis(aminophenol) and B benzoxazaborole is linked through the benzene diboronic acid.

## CHAPTER III

### Conclusions

The main goal of this work was to synthesize macrocycles based on oligo(benzoxazaborole)s using alkyl-linked bis(aminophenol)s, and subsequently, study the ring chain equilibrium of the products. The synthesis of alkyl-linked bis and oligo(benzoxazaborole)s is possible under mild conditions, such as simple mixing and refluxing in toluene. When the starting materials are mixed in CDCl<sub>3</sub>, the solubility of the bis(benzoxazaborole) in CDCl<sub>3</sub> is the key factor to drive the reaction forward even the starting material is not completely soluble. The synthesis of alkyl-linked bis(benzoxazaborole)s in DMSO-*d*<sub>6</sub> and THF-*d*<sub>8</sub> was limited due to the instability of the product due to the presence of water. However, these solvents can be used to characterize alkyl-linked bis(benzoxazaborole)s.

Characterization of poly(benzoxazaborole)s using <sup>1</sup>H NMR and <sup>13</sup>C NMR was not successful due to the poor solubility of poly(benzoxazaborole)s in common organic solvents. However, polymers **8** and **9** exhibit dynamic covalent nature.

The results from the melting point analysis reveal that the isolated polymers **8** and **9** from both reactions are not simply a mixture of starting materials and it is further evidence of polymer or oligomer formation.

Polymer formation is also supported through IR spectroscopic analysis. The absence of signals for OH and NH functional groups in the region of 3200-3600 cm<sup>-1</sup> supports the consumption of the starting materials and formation of the benzoxazaborole moiety. This also suggests macrocycle formation or a high degree of polymerization.

Finally, the initial results from the thermodynamic calculations predict that the formation of benzoxazaboroles depend on the difference in the connectivity of the benzoxazaborole rings within the structure. The structures were found to be less stable when they consist of a bis(benzoxazaborole) that is connected to the 1,4 positions on the benzene ring of benzene diboronic acid (B linkage), which is likely due to the conjugation. Additionally, the linear benzoxazaboroles are more favorable than the ring structures, but the energy difference is minimal.

In the future, further characterization of the polymers **8** and **9** should be carried out to identify the structure of the products. Additional synthesis of bis(aminophenol) derivatives should be explored to synthesize more soluble poly(benzoxazaboroles)s and therefore be able to study the ring-chain equilibrium experimentally.

## CHAPTER IV

### Experimental Section

**Chemicals and Reagents.** All starting materials and reagents were purchased from commercial sources (Acros, Alfa Aesar, MagniSolv, and Ark Pham, Inc.) and used without further purification unless otherwise mentioned. NMR solvents ( $\text{CDCl}_3$ ,  $\text{DMSO-}d_6$ ,  $\text{THF-}d_8$ ) were stored over 4 Å molecular sieves or obtained from a freshly opened ampule.

**Chromatography.** All thin layer chromatography (TLC) analyses were performed on silica gel 60 F<sub>254</sub> aluminum sheets and corresponding visualizations were carried out with UV light (254 nm). Column chromatographic separations were conducted using 60 Å silica gel.

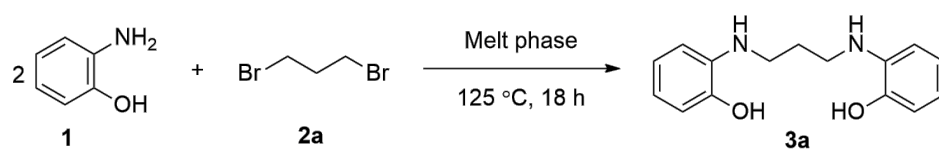
**NMR Spectroscopy.** The  $^1\text{H}$  and  $^{13}\text{C}$  spectra were collected on a JEOL Eclipse 300+ spectrometer. Chemical shifts are reported in  $\delta$  (ppm) relative to the solvent signal for  $^1\text{H}$  and  $^{13}\text{C}$  {( $\text{CHCl}_3$ : 7.25 for  $^1\text{H}$  and 77.23 for  $^{13}\text{C}$ ), ( $\text{DMSO-}d_6$ : 2.47 for  $^1\text{H}$  and 39.52 for  $^{13}\text{C}$ ), or ( $\text{THF-}d_8$ : 3.55 and 1.70 for  $^1\text{H}$ ; and 67.57 and 25.37 for  $^{13}\text{C}$ )}. The splitting patterns are designated as s (singlet); d (doublet); t (triplet); q (quartet); p (pentet); m (multiplet). (See Appendix A for the complete spectra for all new synthesized compounds.)

**FTIR Spectroscopy.** FTIR spectra were collected using a Nicolet iS10 spectrophotometer equipped with the Smart iTX diamond ATR accessory. The spectra were automatically adjusted for  $\text{H}_2\text{O}$ ,  $\text{CO}_2$ , and background corrections. The spectra were plotted with percent transmittance versus wavenumber ( $\text{cm}^{-1}$ ).

**Computational Chemistry.** All calculations of were performed with the Gaussian G09w suite of programs. Initially, the molecular structures were built within the GaussView 5.0 interface and the geometric optimization was carried out in the gas phase

using the molecular mechanics/UFF method. Then, the optimized geometries were subjected to optimization at the semi-empirical level using the PM3 method to obtain geometries with the lowest energy. Finally, the structure resulting from the PM3 calculations were subjected to geometry optimization using the Hartree-Fock (HF) method with a minimal basis set (3-21 G) to obtain more accurate geometries, and subsequently, the frequencies were calculated using that same level of theory. The Gibbs free energies of formation ( $\Delta G_{\text{formation}}$ ) of possible cyclic and acyclic oligo(benzoxazaboroles)s (**8a-g** and **9a-g**) were calculated in the gas phase at room temperature (298 K) using the equation  $\Delta G_{\text{formation}} = E_{\text{products}} - E_{\text{reactants}}$ . Next, the  $\Delta G_{\text{formation}}$  per oxazaborole ring was calculated by dividing the  $\Delta G_{\text{formation}}$  for the reaction by the number of borole rings in that particular structure to compare the relative stability of the oligo(benzoxazaborole)s. The structures that have more than one oxazaborole ring (**8b-g** and **9b-g**) are expected to have a  $\Delta G_{\text{formation}}$  equal to that of the product of number of borole rings multiplied by the  $\Delta G_{\text{formation}}$  of the simple benzoxazaborole 1+1 (**8a** and **9a**).

### Synthesis of propane-1,3-bis(aminophenol) (**3a**)

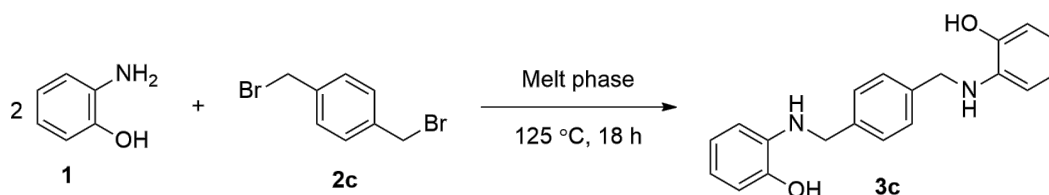


A mixture of 2-aminophenol (2.15 g, 19.7 mmol, 2 equiv) and 1,3-dibromopropane (1.0 mL, 9.81 mmol, 1 equiv) were placed in a sealed tube and heated in an oil bath at 125 °C for 18 h. The mixture was cooled to room temperature. Sodium hydroxide (10 M, 10 mL), brine (sat. NaCl, 10 mL), and ethyl acetate (EtOAc, 30 mL) were added, and the mixture was sonicated for several hours until all solids were suspended. The resulting mixture was extracted with several portions of EtOAc (6x20 mL), and the combined

organic layers (150 mL in total) were dried with anhydrous sodium sulfate ( $\text{Na}_2\text{SO}_4$ ). A TLC was run for the organic phase [EtOAc:hexanes (1:2)]. The product had an apparent  $R_f = 0.26$ . The volatiles were evaporated and using a rotary evaporator to obtain the crude product.

EtOAc (200 mL) and silica 20 mL were added to the crude product and mixed well. Then the resulting dark brown mixture was rotary evaporated and placed under high vacuum to remove the EtOAc. The dried sample was then loaded onto a silica gel-packed column and purified by column chromatography [silica gel, EtOAc:hexanes (1:2)]. This product was purified further by washing with chloroform to obtain a tan solid (633 mg, 25% yield). M.p. = 157-159 (dec.). The  $^1\text{H}$  NMR matched the literature.<sup>43</sup>  $^1\text{H}$  NMR (301 MHz, DMSO-*d*<sub>6</sub>,  $\delta$ ): 9.15 (1H, s, OH), 6.62-6.33 (4H, m, ArH), 4.60-4.56 (1H, t, NH), 3.12-3.06 (4H, d, NH-CH<sub>2</sub>), 1.82-1.78 (2H, m, CH<sub>2</sub>-CH<sub>2</sub>-CH<sub>2</sub>). IR (ATR)  $\nu = 3356, 3315 \text{ cm}^{-1}$ .

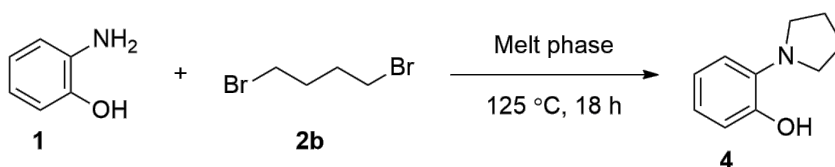
### Synthesis of p-xylylene-1,4-bis(aminophenol) (3c)



A mixture of 2-aminophenol (1.08 g, 9.85 mmol, 2 equiv) and 1,4-bis(bromomethyl)benzene (1.30 g, 4.93 mmol, 1 equiv) were placed in a sealed tube and heated in an oil bath at 125 °C for 18 h. The mixture was cooled down to room temperature and crude product was transferred to an Erlenmeyer flask. A NaOH solution (10 M, 10 mL), methanol (10 mL), sat. NaCl (10 mL), and EtOAc (30 mL) were added, and the mixture was sonicated for several hours until all the solids were suspended. The resulting

mixture was extracted with several portions of EtOAc (6x20 mL), and the combined organic layer (150 mL in total) was dried with anhydrous Na<sub>2</sub>SO<sub>4</sub>. Silica (20 mL) was added to the mixture and it was rotary evaporated to remove EtOAc and obtain a dried sample coated with silica. The dried sample was loaded onto a silica gel-packed column and purified by column chromatography [silica gel, ethyl acetate:hexanes (1:3)] to obtain a white solid. The solid precipitated from the column fractions and was isolated by filtration (79 mg, 5% yield). M.p. = 205-206 (dec.) <sup>1</sup>H NMR and <sup>13</sup>C NMR were obtained to identify and check the purity of the product. <sup>1</sup>H NMR (301 MHz, THF-*d*<sub>8</sub>, δ): 8.08 (1H, s, OH), 7.29 (4H, s, ArH), 6.55-6.32 (4H, m, ArH), 4.78-4.74 (1H, t, NH), 4.28-4.26 (4H, d, NH-CH<sub>2</sub>). <sup>13</sup>C NMR (76 MHz, DMSO-*d*<sub>6</sub>, δ): 144.6 (2C, Ar-C), 139.4 (2C, Ar-C), 137.7 (2C, Ar-C), 127.6 (4C, Ar-C), 120.1 (2C, Ar-C), 116.3 (2C, Ar-C), 113.9 (2C, Ar-C), 110.6 (2C, Ar-C), 46.9 (2C). IR (ATR) ν = 3320 cm<sup>-1</sup>.

#### Attempted Synthesis of butane-1,4-bis(aminophenol) (3b)

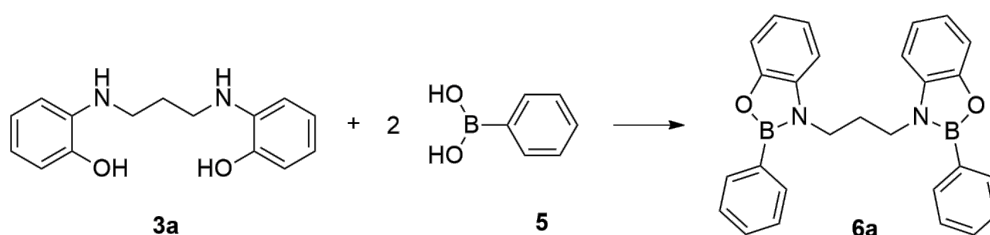


A mixture of 2-aminophenol (1.83 g, 16.74 mmol, 2 equiv) and 1,4-dibromobutane (1.0 mL, 8.37 mmol, 1 equiv) were placed in a sealed tube and heated in an oil bath at 125 °C for 18 h. The mixture was cooled to room temperature. NaOH solution (10 M, 10 mL), sat. NaCl (10 mL), and EtOAc (30 mL) were added and sonicated for several hours until the solids were suspended. The resulting mixture was extracted with several portions of EtOAc (6x20 mL). The combined organic layer (150 mL) was dried with anhydrous Na<sub>2</sub>SO<sub>4</sub> and the organic layer was rotary evaporated to remove EtOAc and obtain the crude

product.  $^1\text{H-NMR}$  was obtained to identify the crude product and was determined to be a pyrrolidine product.

However, EtOAc about (20 mL) was added to the crude product and dissolved all the solids. The small amount of resulting dark red-brown mixture was purified by column chromatography [silica gel, ethyl acetate:hexanes (1:1)] to obtain white color solid. The  $^1\text{H}$  NMR was run to check the purity of the product.  $^1\text{H}$  NMR (301 MHz,  $\text{CDCl}_3$ ,  $\delta$ ): 7.14-6.81 (4H, m, ArH), 3.03-2.99 (4H, t, N- $\text{CH}_2$ ), 2.00-1.93 (4H, q,  $\text{CH}_2$ ).

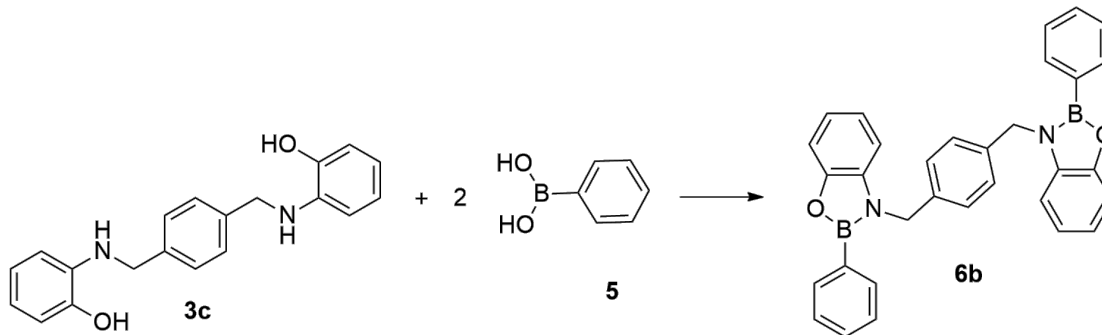
### Propane-1,3-bis(benzoxazaborole) (**6a**)



The direct formation of bis(benzoxazaborole) **6a** was attempted by mixing phenylboronic acid (**5**) (4.3 mg, 0.036 mmol, 2 equiv) and propane-1,3-bis(aminophenol) (**3a**) (4.6 mg, 0.018 mmol, 1 equiv) in  $\text{CDCl}_3$  in an NMR tube.  $^1\text{H}$  NMR (301 MHz,  $\text{CDCl}_3$ ,  $\delta$ ): 7.79-7.76 (4H, d, ArH), 7.45-7.33 (6H, m, ArH), 7.33-7.30 (2H, m, ArH), 7.09-6.96 (6H, m, ArH), 4.04-4.02 (4H, t, N- $\text{CH}_2$ ), 2.41-2.33 (2H, p,  $\text{CH}_2\text{-CH}_2\text{-CH}_2$ ).

The milligram-scale synthesis was achieved, by loading a 50 mL round bottom flask with propane-1,3-bis(aminophenol) (**3a**) (32.3 mg, 0.125 mmol, 1 equiv) and phenylboronic acid (**5**) (30.5 mg, 0.250 mmol, 2 equiv) in toluene (15.0 mL) and refluxing for 9 h with a Dean-Stark trap. The solvent was removed under vacuum at room temperature to give a pale brown solid (33 mg, 62%).<sup>43</sup>  $^1\text{H}$  NMR (301 MHz,  $\text{CDCl}_3$ ,  $\delta$ ): 7.79-7.76 (4H, d, ArH), 7.45-7.33 (6H, m, ArH), 7.33-7.30 (2H, m, ArH), 7.09-6.96 (6H, m, ArH), 4.04-4.02 (4H, t, N- $\text{CH}_2$ ), 2.41-2.33 (2H, p,  $\text{CH}_2\text{-CH}_2\text{-CH}_2$ ).

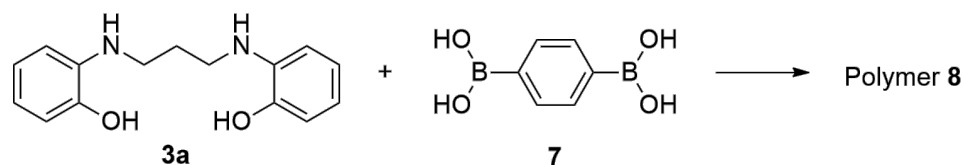
**p-Xylylene-1,4-bis(benzoxazaborole) (6b)**



The direct formation of bis(benzoxazaborole) **6b** was attempted by mixing phenylboronic acid (**5**) (2.4 mg, 0.02 mmol, 2 equiv) and p-xylylene bis(aminophenol) (**3c**) (3.2 mg, 0.01 mmol, 1 equiv) in CDCl<sub>3</sub> or THF-*d*<sub>8</sub> in an NMR tube. <sup>1</sup>H NMR (301 MHz, CDCl<sub>3</sub>, δ): 7.87-7.85 (4H, d, ArH), 7.53-7.42 (6H, m, ArH), 7.33-7.30 (2H, m, ArH), 7.22 (4H, s, ArH), 7.02-6.81 (6H, m, ArH), 5.11 (4H, s, N-CH<sub>2</sub>). <sup>1</sup>H NMR (301 MHz, THF-*d*<sub>8</sub>, δ): 7.88-7.86 (4H, d, ArH), 7.42-7.32 (8H, m, ArH), 7.25 (4H, s, ArH), 7.95-6.92 (6H, m, ArH), 5.15 (4H, s, N-CH<sub>2</sub>).

Next, for the synthesis of bis(benzoxazaborole) **6b**, p-xylylene bis(aminophenol) (**3c**) (9.5 mg, 0.03 mmol, 1 equiv) toluene (6.0 mL) were added to a 20 mL reaction vial and stirred at 60 °C for five minutes. Then phenylboronic acid (**5**) (6.5 mg, 0.06 mmol, 2 equiv) was added and left to stir for 5 hours. The solvent was removed under vacuum at room temperature to give a yellow solid (21.3 mg). <sup>1</sup>H NMR (301 MHz, THF-*d*<sub>8</sub>, δ): 7.89-7.87 (4H, d, ArH), 7.51-7.40 (6H, m, ArH), 7.36-7.31 (2H, m, ArH), 7.25 (4H, s, ArH), 7.04-6.86 (6H, m, ArH), 5.12 (4H, s, N-CH<sub>2</sub>). <sup>13</sup>C NMR (76 MHz, CDCl<sub>3</sub>, δ): 149.5 (2C, Ar-C), 138.5 (2C, Ar-C), 137.2 (2C, Ar-C), 134.1 (4C, Ar-C), 130.8 (2C, Ar-C), 128.4 (6C, Ar-C), 126.9 (4C, Ar-C), 122.0 (2C, Ar-C), 120.6 (2C, Ar-C), 112.4 (2C, Ar-C), 110.3 (2C, Ar-C), 46.6 (2C).

**Propane-1,3-poly(benzoxazaborole) (8)**

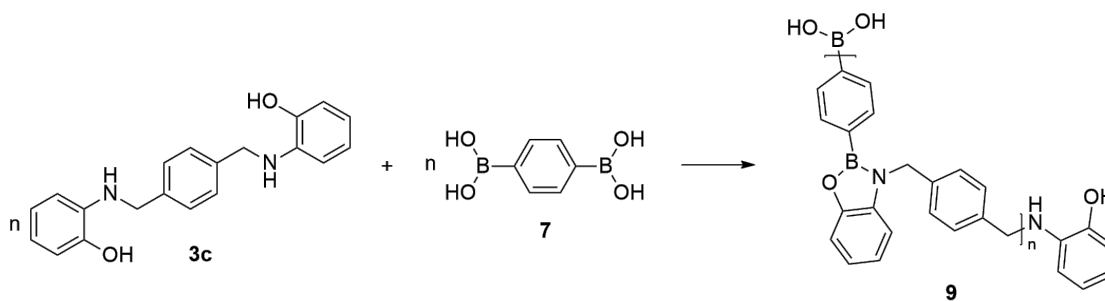


The direct formation of poly(benzoxazaborole) **8** was attempted by mixing propane-1,3-bis(aminophenol) (**3a**) (4.6 mg, 0.018 mmol, 1 equiv) and benzene diboronic acid (**7**) (3.0 mg, 0.018 mmol, 1 equiv) in DMSO-*d*<sub>6</sub> in an NMR tube.

Next, the synthesis of poly(benzoxazaborole) **8** was attempted by mixing propane-1,3-bis(aminophenol) (**3a**) (10.0 mg, 0.039 mmol, 1 equiv) and phenylboronic acid (**5**) (6.5 mg, 0.06 mmol, 2 equiv) in a 20 mL reaction vial with EtOAc (7 mL). The reaction mixture was stirred for 30 minutes. The solvent was removed under vacuum at room temperature to give a white solid. The vial was connected to the vacuum line to remove excess solvent. The product did not dissolve in CDCl<sub>3</sub> and no signals were present in the <sup>1</sup>H NMR spectrum.

Finally, the same synthesis was attempted in a 50 mL round bottom flask, by mixing propane-1,3-bis(aminophenol) (**3a**) (32.3 mg, 0.125 mmol, 1 equiv) and benzene diboronic acid (**7**) (20.7 mg, 0.125 mmol, 1 equiv) in toluene (50 mL) and ethanol (4 mL) and refluxed overnight with a Dean-Stark trap. The white product was crystallized upon cooling. The supernatant was removed using a pipette. Two fractions were rotary evaporated at room temperature to remove excess solvent and to give a white solid (30 mg, 68%). M.p. = 325-326 (dec.). Attempts were made to analyze the product by <sup>1</sup>H NMR but it did not dissolve in solvents such as chloroform, dimethyl sulfoxide, tetrahydrofuran, acetone, dichloromethane, ethyl acetate, N,N-dimethylformamide, ethanol, acetonitrile, and water.

**p-Xylylene poly(benzoxazaborole) (9)**



Direct formation of poly(benzoxazaborole) **9** was attempted by mixing p-xylylene bis(aminophenol) (**3c**) (3.2 mg, 0.01 mmol, 1 equiv) and benzene diboronic acid (**7**) (1.7 mg, 0.01 mmol, 1 equiv) in DMSO-*d*<sub>6</sub> and in THF-*d*<sub>8</sub> in an NMR tube. The <sup>1</sup>H NMR showed evidence of benzoxazaborole formation immediately after mixing the starting materials, which did not increase significantly over time.

Next, for the synthesis of poly(benzoxazaborole) **9**, p-xylylene bis(aminophenol) (**3c**) (8.0 mg, 0.025 mmol, 1 equiv) was measured to a 20 mL reaction vial and toluene (5.0 mL) and ethanol (1.0 mL) were added and stirred at 60 °C for 10 minutes. Then benzene diboronic acid (**7**) (4.1 mg, 0.025 mmol, 1 equiv) was added and let to stir for another 20 minutes. Then the vial was cooled to room temperature. The solvent was removed under vacuum at room temperature to give a white solid. The vial was connected to the vacuum line to remove excess solvent. (11.8 mg, 22.7%). The product was analyzed by <sup>1</sup>H NMR. Most of the sample remained undissolved and spectrum had new signals at 7.50-6.75 δ (ppm) that would be expected for benzoxazaborole formation.

The same for the same synthesis, p-xylylene bis(aminophenol) (**3c**) (40.0 mg, 0.125 mmol, 1 equiv) and benzene diboronic acid (**7**) (20.7 mg, 0.125 mmol, 1 equiv) were mixed in toluene (50 mL) and ethanol (5 mL) in a 50 mL round bottom flask. The mixture was refluxed overnight with a Dean-Stark trap. The white product was crystallized upon

cooling. The supernatant was removed using a pipette. Two fractions were rotary evaporated at room temperature to remove excess solvent and to give a white solid. (40 mg, 77%). M.p. = 364-366 (dec.). Attempts were made to analyze the product by  $^1\text{H}$  NMR but it did not dissolve in solvents such as  $\text{CDCl}_3$ ,  $\text{DMSO-}d_6$ ,  $\text{THF-}d_8$ , acetone, DCM, benzene, hexane, acetonitrile, and in DMF and water. Then polymer **9** was added to an NMR tube containing  $\text{DMSO-}d_6$  with a drop of water. It was heated at 90 °C and analyzed over time see any change in the  $^1\text{H}$  NMR. After 24 hours, the  $^1\text{H}$  NMR showed the signals for the starting materials.

## REFERENCES

- (1) Schaufelberger, F.; Timmer, B. J. J.; Ramström, O. Dynamic Covalent Chemistry. In *Principles of Dynamic Covalent Chemistry*; Zang, W., Jin, Y., Eds.; John Wiley & Sons Ltd.: Hoboken, NJ, 2018; pp 9–22.
- (2) Wojtecki, R. J.; Meador, M. A.; Rowan, S. J. Using the dynamic bond to access macroscopically responsive structurally dynamic polymers. *Nat. Mater.* **2011**, *10*, 14–27.
- (3) Nowak, P.; Saggiomo, V.; Salehian, F.; Colomb-Delsuc, M.; Han, Y.; Otto, S. Localized template-driven functionalization of nanoparticles by dynamic combinatorial chemistry. *Angew. Chem. Int. Ed.* **2015**, *54*, 4192–4197.
- (4) Dydio, P.; Breuil, P. A. R.; Reek, J. N. H. Dynamic combinatorial chemistry in chemical catalysis. *Isr. J. Chem.* **2013**, *53*, 61–74.
- (5) Tauk, L.; Schröder, A. P.; Decher, G.; Giuseppone, N. Hierarchical functional gradients of pH-responsive self-assembled monolayers using dynamic covalent chemistry on surfaces. *Nat. Chem.* **2009**, *1*, 649–656.
- (6) Serafimova, I. M.; Pufall, M. A.; Krishnan, S.; Duda, K.; Cohen, M. S.; Maglathlin, R. L.; McFarland, J. M.; Miller, R. M.; Frödin, M.; Taunton, J. Reversible targeting of noncatalytic cysteines with chemically tuned electrophiles. *Nat. Chem. Biol.* **2012**, *8*, 471–476.
- (7) Aida, T.; Meijer, E. W.; Stupp, S. I. Functional supramolecular polymers. *Science* **2012**, *335*, 813–817.
- (8) Zhang, W.; Moore, J. S. Shape-Persistent Macrocycles: Structures and Synthetic Approaches from Arylene and Ethynylene Building Blocks. *Angew. Chem. Int. Ed.*

- 2006**, *45*, 4416–4439.
- (9) Hodge, P. Recycling of condensation polymers via ring-chain equilibria. *Polym. Adv. Technol.* **2015**, *26*, 797–803.
- (10) Jin, Y.; Yu, C.; Denman, R. J.; Zhang, W. Recent Advances in Dynamic Covalent Chemistry. *Chem. Soc. Rev.* **2013**, *42*, 6634–6654.
- (11) Schaufelberger, F.; Timmer, B. J. J.; Ramström, O. Principles of Dynamic Covalent Chemistry. In *Dynamic Covalent Chemistry*; Jin, Y., Zhang, W., Eds.; Wiley-VCH: Weinheim, 2017; pp 1–30.
- (12) Zou, W.; Dong, J.; Luo, Y.; Zhao, Q.; Xie, T. Dynamic Covalent Polymer Networks: from Old Chemistry to Modern Day Innovations. *Adv. Mater.* **2017**, *29*, 1–18.
- (13) Rekondo, A.; Martin, R.; Ruiz De Luzuriaga, A.; Cabañero, G.; Grande, H. J.; Odriozola, I. Catalyst-free room-temperature self-healing elastomers based on aromatic disulfide metathesis. *Mater. Horizons* **2014**, *1*, 237–240.
- (14) Schaufelberger, F.; Seigel, K.; Ramström, O. Hydrogen-Bond Catalysis of Imine Exchange in Dynamic Covalent Systems. *Chem. Eur. J.* **2020**, *26*, 15581–15588.
- (15) James, T. D.; Sandanayake, K. R. A. S.; Shinkai, S. Saccharide sensing with molecular receptors based on boronic acid. *Angew. Chem. Int. Ed.* **1996**, *35*, 1910–1922.
- (16) Wang, W.; Gao, X.; Wang, B. Boronic Acid-Based Sensors. *Curr. Org. Chem.* **2002**, *6*, 1285–1317.
- (17) Iwasawa, N.; Takahagi, H. Boronic Esters as a System for Crystallization-Induced Dynamic Self-Assembly Equipped with an “On–Off” Switch for Equilibration. *J.*

- Am. Chem. Soc.* **2007**, *129*, 7754–7755.
- (18) Takahagi, H.; Fujibe, S.; Iwasawa, N. Guest-induced dynamic self-assembly of two diastereomeric cage-like boronic esters. *Chem. Eur. J.* **2009**, *15*, 13327–13330.
- (19) Cromwell, O. R.; Chung, J.; Guan, Z. Malleable and Self-Healing Covalent Polymer Networks through Tunable Dynamic Boronic Ester Bonds. *J. Am. Chem. Soc.* **2015**, *137*, 6492–6495.
- (20) Christinat, N.; Croisier, E.; Scopelliti, R.; Cascella, M.; Röthlisberger, U.; Severin, K. Formation of Boronate Ester Polymers with Efficient Intrastrand Charge-Transfer Transitions by Three-Component Reactions. *Eur. J. Inorg. Chem.* **2007**, *2007*, 5177–5181.
- (21) Côté, A. P.; El-Kaderi, H. M.; Furukawa, H.; Hunt, J. R.; Yaghi, O. M. Reticular Synthesis of Microporous and Mesoporous 2D Covalent Organic Frameworks. *J. Am. Chem. Soc.* **2007**, *129*, 12914–12915.
- (22) Côté, A. P.; Benin, A. I.; Ockwig, N. W.; O’Keeffe, M.; Matzger, A. J.; Yaghi, O. M. Porous, Crystalline, Covalent Organic Frameworks. *Science* **2005**, *310*, 1166–1170.
- (23) Smith, M. K.; Powers-Riggs, N. E.; Northrop, B. H. Discrete, soluble covalent organic boronate ester rectangles. *Chem. Commun.*, **2013**, *49*, 6167–6169.
- (24) Zhang, X.; Wang, S.; Jiang, Z.; Li, Y.; Jing, X. Boronic Ester Based Vitrimers with Enhanced Stability via Internal Boron-Nitrogen Coordination. *J. Am. Chem. Soc.* **2020**, *142*, 21852–21860.
- (25) Christinat, N.; Scopelliti, R.; Severin, K. Multicomponent assembly of boron-

- based dendritic nanostructures. *J. Org. Chem.* **2007**, *72*, 2192–2200.
- (26) Zhu, L.; Zhang, Y.-B. Crystallization of Covalent Organic Frameworks for Gas Storage Applications. *Molecules* **2017**, *22*, 1149–1168.
- (27) Wan, S.; Guo, J.; Kim, J.; Ihee, H.; Jiang, D. A belt-shaped, blue luminescent, and semiconducting covalent organic framework. *Angew. Chem. Int. Ed.* **2008**, *47*, 8826–8830.
- (28) Wan, S.; Guo, J.; Kim, J.; Ihee, H.; Jiang, D. A Photoconductive Covalent Organic Framework : Self-Condensed Arene Cubes Composed of Eclipsed 2D Polypyrene Sheets for Photocurrent Generation. *Angew. Chem. Int. Ed.* **2009**, *48*, 5439–5442.
- (29) Dogru, M.; Bein, T. On the road towards electroactive covalent organic frameworks. *Chem. Commun.* **2014**, *50*, 5531–5546.
- (30) Ding, S.-Y.; Gao, J.; Wang, Q.; Zhang, Y.; Song, W.-G.; Su, C.-Y.; Wang, W. Construction of Covalent Organic Framework for Catalysis: Pd/COF-LZU1 in Suzuki–Miyaura Coupling Reaction. *J. Am. Chem. Soc.* **2011**, *133*, 19816–19822.
- (31) Dalapati, S.; Jin, S.; Gao, J.; Xu, Y.; Nagai, A.; Jiang, D. An azine-linked covalent organic framework. *J. Am. Chem. Soc.* **2013**, *135*, 17310–17313.
- (32) Wan, S.; Gándara, F.; Asano, A.; Furukawa, H.; Saeki, A.; Dey, S. K.; Liao, L.; Ambrogio, M. W.; Botros, Y. Y.; Duan, X.; Seki, S.; Stoddart, J. F.; Yaghi, O. M. Covalent Organic Frameworks with High Charge Carrier Mobility. *Chem. Mater.* **2011**, *23*, 4094–4097.
- (33) Christnat, N.; Croisier, E.; Scopelliti, R.; Cascella, M.; Rothlisberger, U.; Severin, K. Formation of Boronate Ester Polymers with Efficient Intrastrand Charge-Transfer Transitions by Three-Component Reactions. *Eur. J. Inorg. Chem.* **2007**,

5177–5181.

- (34) El-Kaderi, H. M.; Hunt, J. R.; Mendoza-Cortés, J. L.; Côté, A. P.; Taylor, R. E.; O’Keeffe, M.; Yaghi, O. M. Designed Synthesis of 3D Covalent Organic Frameworks. *Science* **2007**, *316*, 268–272.
- (35) Waller, P. J.; Gándara, F.; Yaghi, O. M. Chemistry of Covalent Organic Frameworks. *Acc. Chem. Res.* **2015**, *48*, 3053–3063.
- (36) Rambo, B. M.; Tilford, R. W.; Lanni, L. M.; Liu, J.; Lavigne, J. J. Boronate-Linked Materials: Ranging from Amorphous Assemblies to Highly Structured Networks. In *Macromolecules Containing Metal and Metal-Like Elements: Supramolecular and Self-Assembled Metal-Containing Materials*; Azis, A. S. A.-E., Carraher, C. E., Pittman, C. U., Zeldin, M., Eds.; John Wiley & Sons, Inc.: Hoboken, NJ, 2009; pp 255–294.
- (37) Weber, L.; Bohling, L. The role of 2,3-dihydro-1-H-1,3,2-diazaboroles in luminescent molecules. *Coord. Chem. Rev.* **2015**, *284*, 236–275.
- (38) Niu, W.; O’Sullivan, C.; Rambo, B. M.; Smith, M. D.; Lavigne, J. J. Self-repairing polymers: poly(dioxaborolane)s containing trigonal planar boron. *Chem. Commun.* **2005**, 4342–4344.
- (39) Mulvaney, J. E.; Bloomfield, J. J.; Marvel, C. S. Polybenzborimidazolines. *J. Polym. Sci.* **1962**, *62*, 59–72.
- (40) Steinberg, H; Brotherton, R. J. Direct Preparation of Some Cyclic Boron-Nitrogen Compounds from Alkoxyboranes. *J. Org. Chem.* **1961**, *26*, 4632–4634.
- (41) Rathnayaka, R. M. C. Synthesis, Characterization, and Computational Studies of 3-Alkylbenzoxazaboroles. M.S. Thesis, Sam Houston State University, Huntsville,

TX, 2018.

- (42) George, S. Synthesis and Characterization of Benzoxazaboroles. M.S. Thesis, Sam Houston State University, Huntsville, TX, 2016.
- (43) Barba, V.; Rodríguez, A.; Ochoa, M. E.; Santillan, R.; Farfán, N. Bisoxazaborolidines and boron complexes derived from tetradentate ligands: synthesis and spectroscopic studies. *Inorg. Chim. Acta* **2004**, *357*, 2593–2601.
- (44) Ochoa, M. E.; Rojas-Lima, S.; Höpfl, H.; Rodríguez, P.; Castillo, D.; Farfán, N.; Santillan, R. Facile synthesis of 1,3,6-oxadiazepines from 2,2'-(1,2-ethanediyl-diimino)bisphenols. *Tetrahedron* **2001**, *57*, 55–64.
- (45) Sellarajah, S.; Lekishvili, T.; Bowring, C.; Thompsett, A. R.; Rudyk, H.; Birkett, C. R.; Brown, D. R.; Gilbert, I. H. Synthesis of analogues of Congo red and evaluation of their anti-prion activity. *J. Med. Chem.* **2004**, *47*, 5515–5534.
- (46) Kombala, C. Investigation of Boronate Ester Equilibria Towards Macrocyclic Synthesis. M.S. Thesis, Sam Houston State University, Huntsville, TX, 2015.
- (47) Drogkaris, V.; Northrop, B. H. Discrete Boronate Ladders from the Dynamic Covalent Self-Assembly of Oligo(phenylene ethynylene) Derivatives and Phenylenebis(boronic acid). *Org. Chem. Front.* **2020**, *7*, 1082–1094.
- (48) Abeysinghe, J. Diazaboroles: Experimental Investigations of their Dynamic Covalent Nature and Computational Chemistry. M.S. Thesis, Sam Houston State University, Huntsville, TX, 2017.

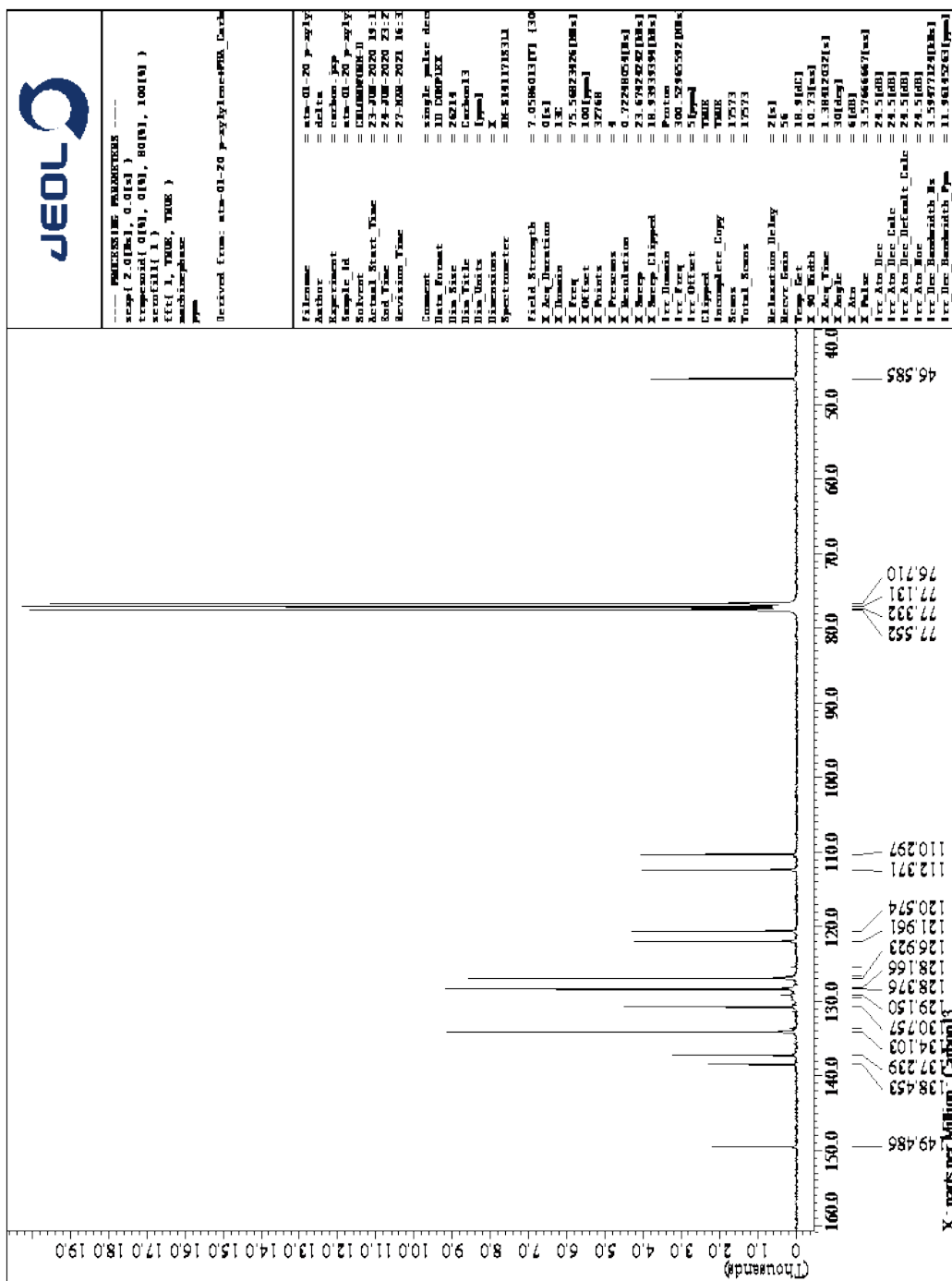








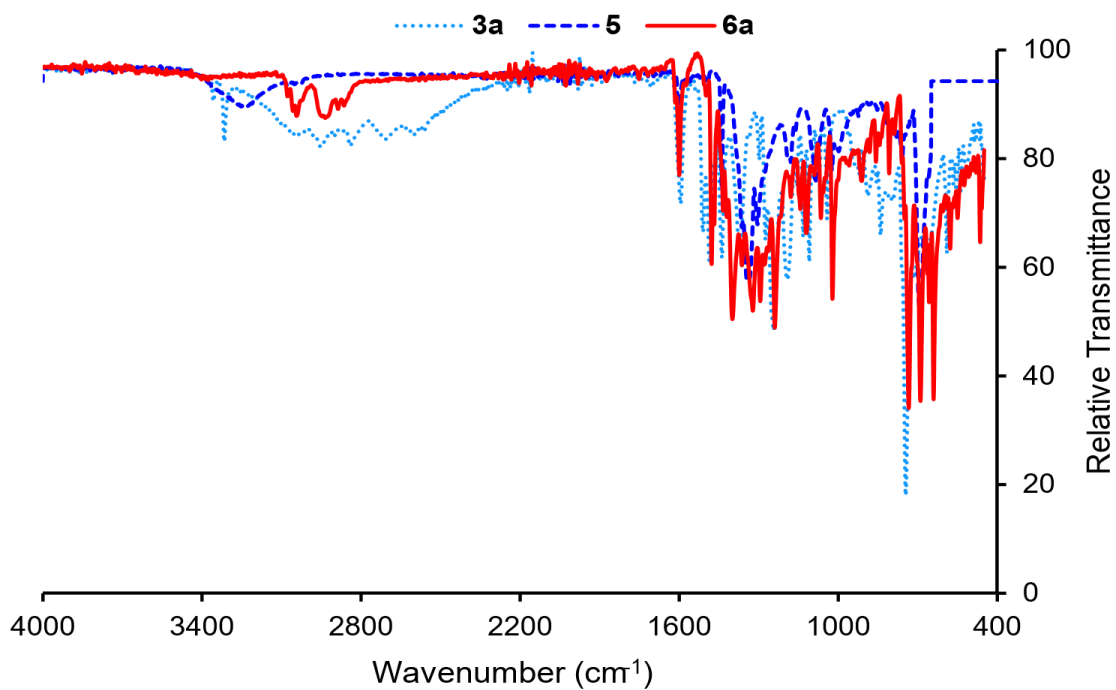




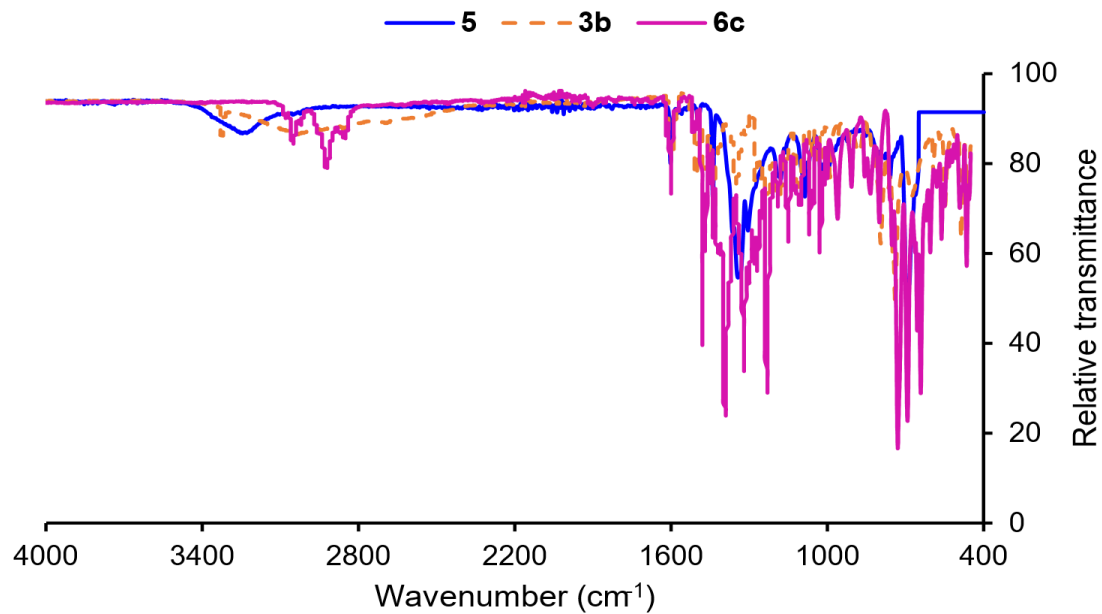
$^{13}\text{C}$  NMR spectrum of p-xylylene linked bis(benzoxazaborole) (**6c**) in  $\text{CDCl}_3$ .

## APPENDIX B

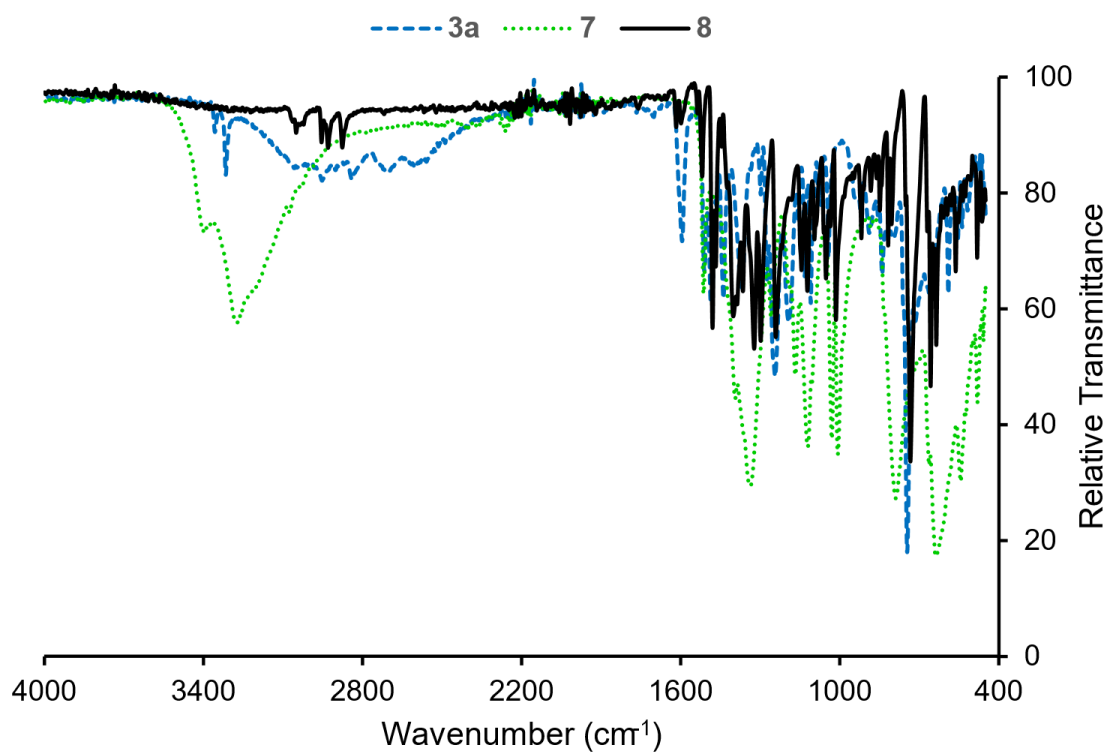
## IR Spectra for the Synthesized Compounds



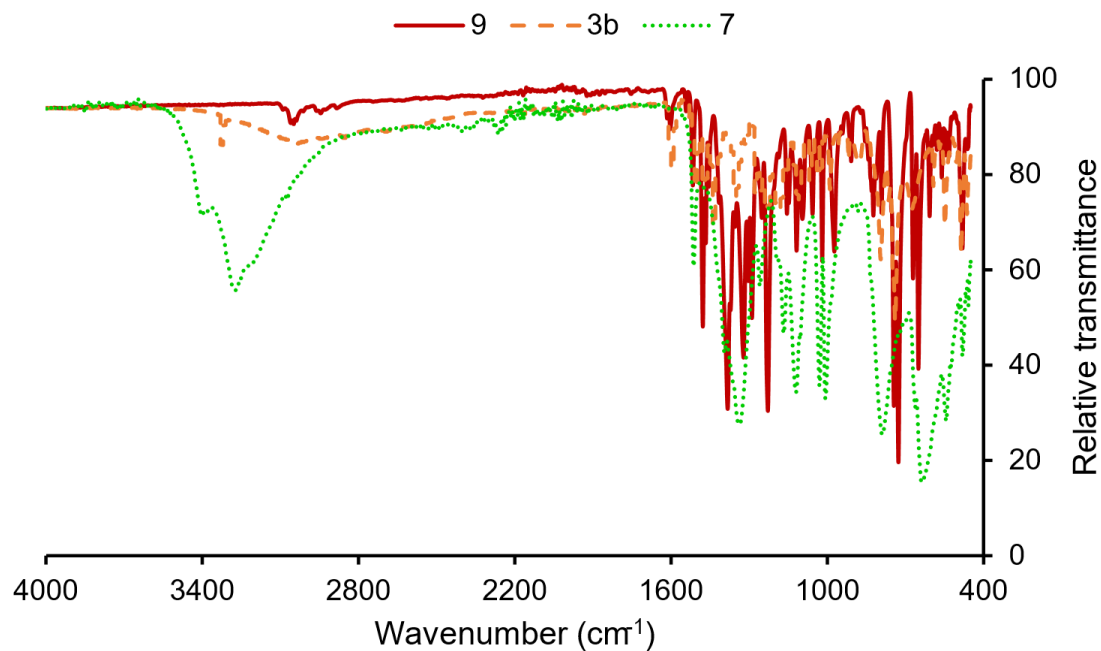
FTIR spectra of propane-1,3-bis(aminophenol) (**3a**), phenylboronic acid (**5**), and propane-1,3-bis(benzoxazaborole) (**6a**).



FTIR spectra of p-xylene bis(aminophenol) (**3c**), phenylboronic acid (**5**), and p-xylene bis(benzoxazaborole) (**6b**).



FTIR spectra of propane-1,3-bis(aminophenol) (**3a**), benzene diboronic acid (**7**), and propane-1,3-poly(benzoxazaborole) (**8**).



FTIR spectra of p-xylylene bis(aminophenol) (**3c**), benzene diboronic acid (**7**), and p-xylylene poly(benzoxazaborole) (**9**).

## VITA

### EDUCATION

**Master of Science in Chemistry** 08/2018 – Present

- *Sam Houston State University, Texas, USA*
- Expected graduation: Spring 2021
- Thesis title: “Investigation of oligo(benzoxazaborole)s derived from alkyl – linked bis(aminophenol)s”
- Advisor: Dr. Dustin E. Gross
- Current GPA: 3.88 out of 4.00

**Bachelor of Science in Chemistry** 03/2013 – 03/2017

- *University of Kelaniya, Sri Lanka*
- Research: “Formulation and characterization of cinnamon leaf oil encapsulated chitosan microcapsules”
- Advisor: Dr. Suranga Wickramarachchi
- GPA: 3.36 out of 4.00

### CONFERENCE AND SYMPOSIUM PRESENTATIONS

- Muthumali A.M.T., Gross D.E., “Bis(aminophenol) derivatives for the synthesis of poly(benzoxazaborole)s and bis(benzoxazaborole)s” Oral presentation at Texas Academy of Science (TAS) Meeting, 2020 (February), Nacogdoches, TX.
- Muthumali A.M.T., Gross D.E., “Synthesis and characterization of poly(benzoxazaborole)s and bis(benzoxazaborole)s derived from bis(aminophenol)s” Poster presented at American Chemical Society (ACS) Southwest Regional Meeting, 2019 (November), El Paso, TX.
- Muthumali A.M.T., Wickramarachchi P.A.S.R., “The effect of changing the oil concentration on oil content, encapsulation efficiency and release rate of cinnamon leaf oil encapsulated chitosan microcapsules” Poster and oral presentation at International Research Symposium on Pure and Applied Sciences, 2017 (October), University of Kelaniya, Sri Lanka.

## TEACHING EXPERIENCE

### Graduate Teaching Assistant

08/2018 – Present

Department of Chemistry, Sam Houston State University

*Instructed and supervised lab courses; graded exams, quizzes, homework problem sets, lab reports, held regular tutoring hours for both lab and lecture courses.*

2018 (fall)	Organic chemistry I laboratory	Dr. Dustin E. Gross
2019 (spring)	Organic chemistry I laboratory	Dr. Dustin E. Gross
2019 (fall)	Organic chemistry I laboratory	Dr. Christopher E. Hobbs
2020 (spring)	Organic chemistry II laboratory	Dr. Christopher E. Hobbs
2020 (fall)	Inorganic and environmental chemistry laboratory	Hemantha, Siyambalagoda, MS
2021 (spring)	Organic chemistry I laboratory General chemistry II laboratory	Dr. Dustin E. Gross Steven Hegwood, MS

### Teaching Assistant

02/2017 – 02/2018

Department of Chemistry, University of Kelaniya, Sri Lanka

*Instructed and supervised lab courses; graded quizzes, homework problem sets, lab reports, preparing chemicals for labs and exams.*

2017 (semester I)	Basic chemical analysis laboratory Introductory organic chemistry laboratory	Prof. Kapila Seneviratne Prof. M.K.B. Weerasooriya
2017 (semester II)	Environmental chemistry laboratory Analytical chemistry laboratory	Prof. Sujeewa De Silva Dr. R.C.L. De Silva

## AWARDS AND MEMBERSHIPS

- College of Science and Engineering Technology Graduate Achievement Scholarship – Fall 2019, Sam Houston State University, TX, USA
- College of Science and Engineering Technology Graduate Achievement Scholarship – Spring 2020, Sam Houston State University, TX, USA
- College of Science and Engineering Technology Graduate Achievement Scholarship – Fall 2020, Sam Houston State University, TX, USA
- Research Scholarship – Part of a grant awarded to Dustin E. Gross – Fall 2019, Sam Houston State University, TX, USA
- Research Scholarship – Part of a grant awarded to Dustin E. Gross – Fall 2020, Sam Houston State University, TX, USA
- Member of Texas Academy of Science

**SKILLS AND COMPETENCIES**

- Lab techniques and instrumentation – Organic synthesis and characterization, NMR, IR spectroscopy, silica gel column chromatography, thin layer column chromatography, melting point, recrystallization, separation
- Software – Microsoft Office, ChemDraw, Mendeley, MestreNova, DELTA, Gaussian g09w